Superconductivity, the pseudogap, and the pairing glue in the 2d Hubbard model

Emanuel Gull

Olivier Parcollet, A.J. Millis

Trieste, Italy

Emanuel Gull and Andrew J. Millis, arXiv:1407.0704

Emanuel Gull, Andrew J. Millis, Olivier Parcollet, Phys. Rev. Lett. 110, 216405 (2013)

Emanuel Gull and Andrew J. Millis, Phys. Rev. B 88, 075127 (2013)

Experiments: Pseudogap

in high-Tc materials: Electronic spectral function is suppressed along the BZ face, but not along zone diagonal.

Key physics dependence on momentum around Fermi surface, Difference of spectral function around Fermi surface.

Doping dependence of region with quasiparticles

ARPES: Shen *et al.*, Science 307, 901 (2005)

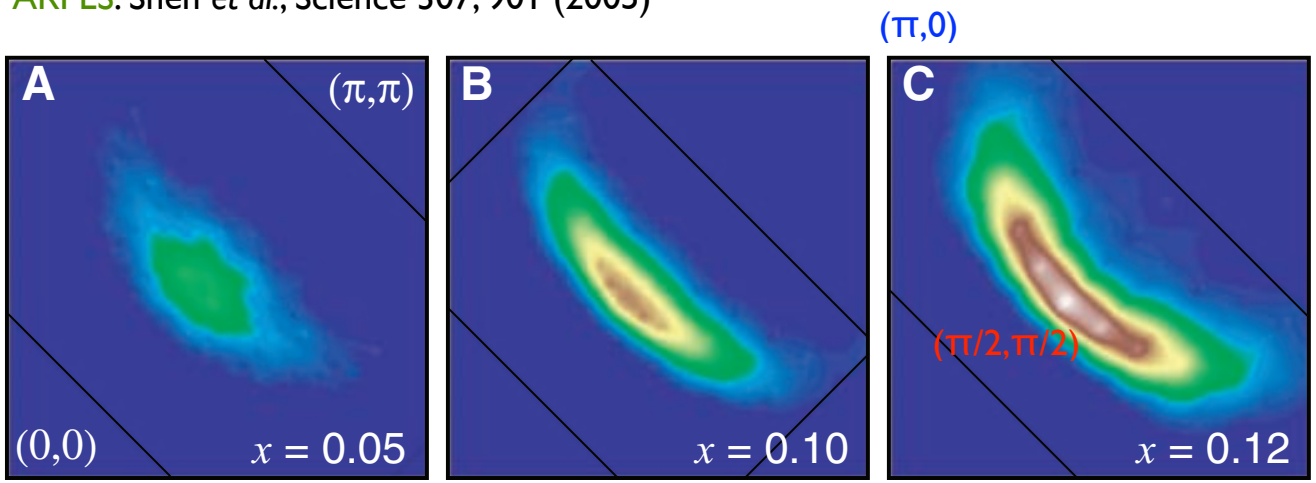

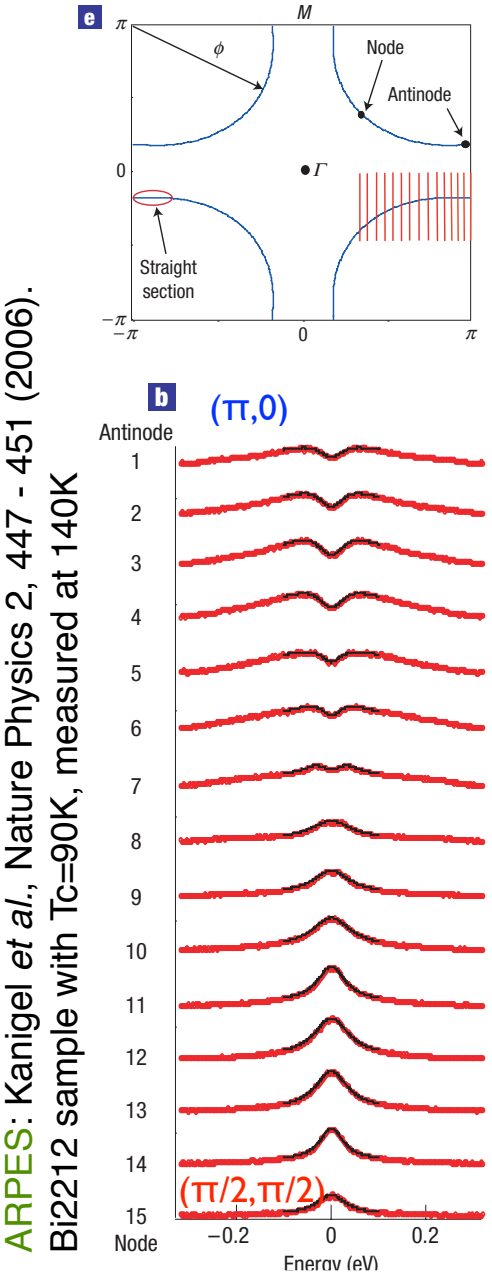

ARPES: Kanigel *et al.*, Nature Physics 2, 447 - 451 (2006). Bi2212 sample with Tc=90K, measured at 140K

Experiments: d-wave superconductivity

Damascelli *et al.*, Rev. Mod. Phys 75, 2 (2003)

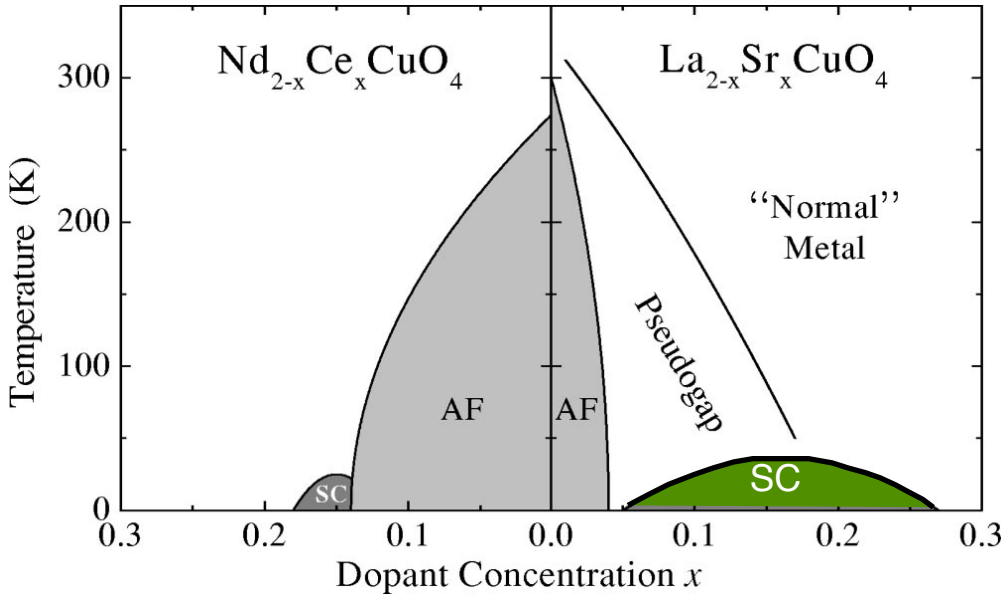

FIG. 1. Phase diagram of n- and p-type superconductors, showing superconductivity (SC), antiferromagnetic (AF), pseudogap, and normal-metal regions.

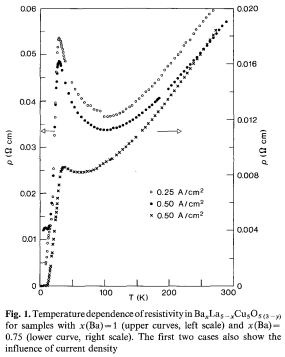

Fig. 1. Temperature dependence of resistivity in $Ba_xLa_{5-3x}Cu_5O_{5(3-y)}$ for samples with $x(Ba)=1$ (upper curves, left scale) and $x(Ba)=0.75$ (lower curve, right scale). The first two cases also show the influence of current density

Bednorz and Müller, Z. Phys. B 64, 189 (1986)

He *et al.*, Science 331, 1579 (2011)

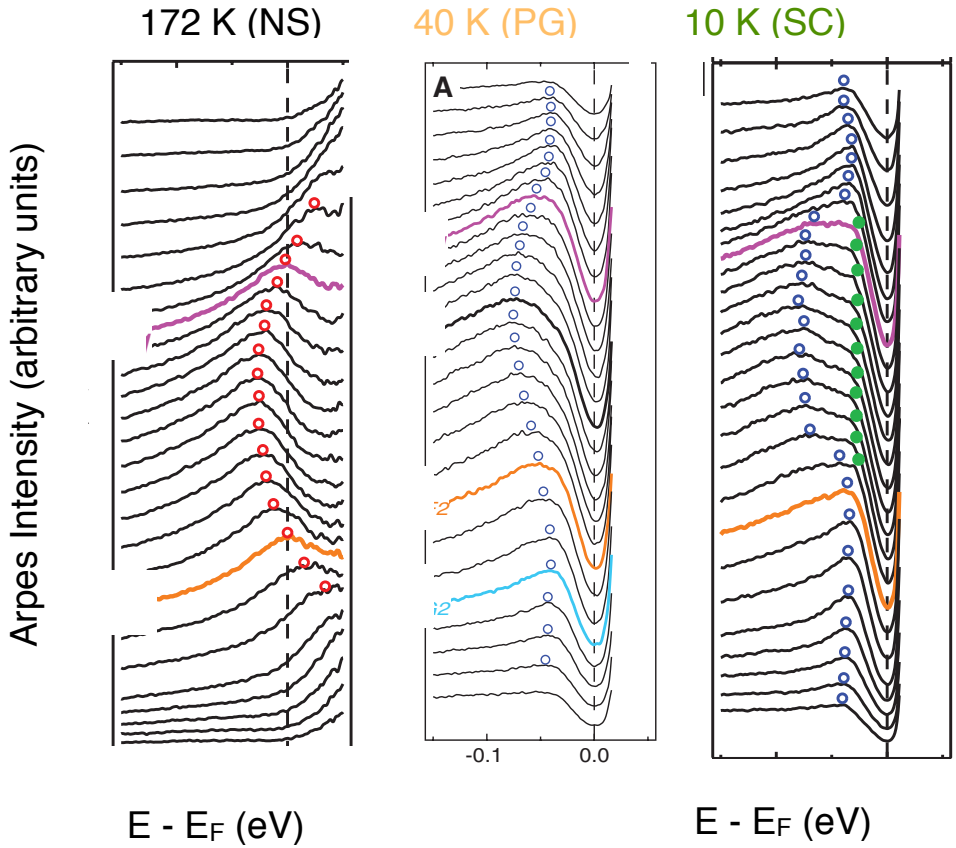

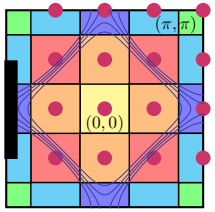

Arpes EDC for cuts along Brillouin-zone boundary (near (π,0)), almost optimally doped Pb-Bi2201 with T_c of 38K. T* of 132K

Questions to theory

Superconductivity at intermediate interaction strengths

Pseudogap at intermediate interaction strengths

Coexistence, precursor, competition, ?

superconducting self energies?

what is the pairing glue?

What is the gap function?

Contained within a well-defined model & systematic and controllable approximation?

……we will present a potential answer in this talk……

Theory: Hubbard model

Restrict to simple minimal model with kinetic and potential energy terms: Hubbard model:

$$H = -\sum_{\langle ij \rangle, \sigma} t_{ij} (c^{\dagger}_{i\sigma} c_{j\sigma} + c^{\dagger}_{j\sigma} c_{i\sigma}) + U \sum_{i} n_{i\uparrow} n_{i\downarrow}.$$

Open theoretical question: **how much of the physics on the last pages is contained in this model?**

Even for the most simple model, when kinetic energy ~ potential energy we have no working theoretical tools: **quantum many-body theory needs numerical methods!**

Here: **Cluster DMFT**: diagrammatic approximation based on mapping of the system onto a self-consistently adjusted multi-orbital quantum impurity model, solved by numerically exact **'continuous-time' QMC**.

Simulations of **wide parameter regimes, for a range of cluster sizes/geometries.** Determine which features are robust, which may be artifacts of the model

Emanuel Gull and Andrew J. Millis, arXiv:1407.0704

Cluster DMFT

Approximation to self energy:

$$\Sigma(k,\omega) = \sum_n \Sigma_n(\omega)\phi_n(k) \approx \sum_n^{N_c} \Sigma_n(\omega)\phi_n(k)$$

← Systematic truncation with cluster size N_c

↑ Basis functions

Cluster DMFT: **controlled** approximation, **exact for $N_c \to \infty$**; 'single site' DMFT for $N_c = 1$. Small parameter $1/N_c$

Example tiling of the BZ: 2d, N_c = 16

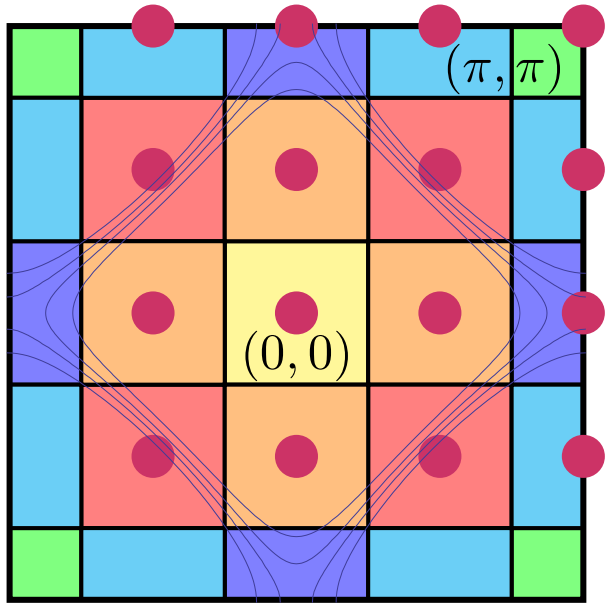

Cluster scheme: 'Dynamical Cluster Approximation' (DCA), basis functions ϕ constant on patches in BZ

Example tiling of the BZ: 2d, N_c = 2, 4, 4, 8

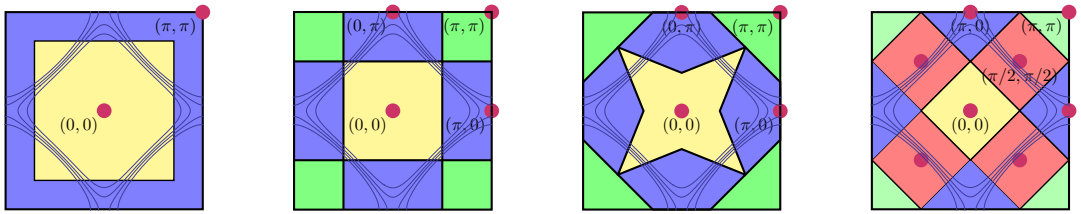

Resulting lattice system mapped onto impurity model & self-consistency

DMFT: Metzner, Vollhardt, Phys. Rev. Lett. 62, 324 (1989), Georges, Kotliar, Phys. Rev. B 45, 6479 (1992), Jarrell, Phys. Rev. Lett. 69, 168 (1992), Georges et al., Rev. Mod. Phys. 68, 13 (1996)

DCA: Hettler et al., Phys. Rev. B 58, R 7475 (1998), Lichtenstein, Katsnelson, Phys. Rev. B 62, R9283 (2000), CDMFT: Kotliar et al., Phys. Rev. Lett. 87, 186401 (2001), Review: T. Maier, et al., Rev. Mod. Phys. 77, 1027 (2005).

Phys. Rev. Lett. 106, 030401 (2011)

Intermezzo: 3D Hubbard Model

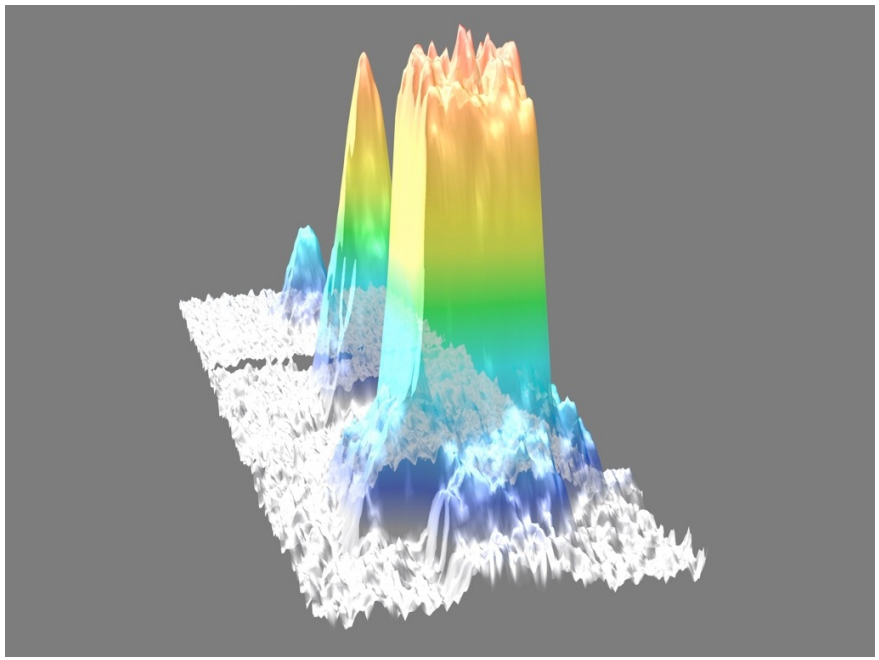

'Optical Lattice Emulator': Goal is to experimentally simulate simple model Hamiltonians using cold atomic (fermionic) gases.

T. Esslinger, Annu. Rev. Condens. Matter Phys. 1, 129-152 (2010)

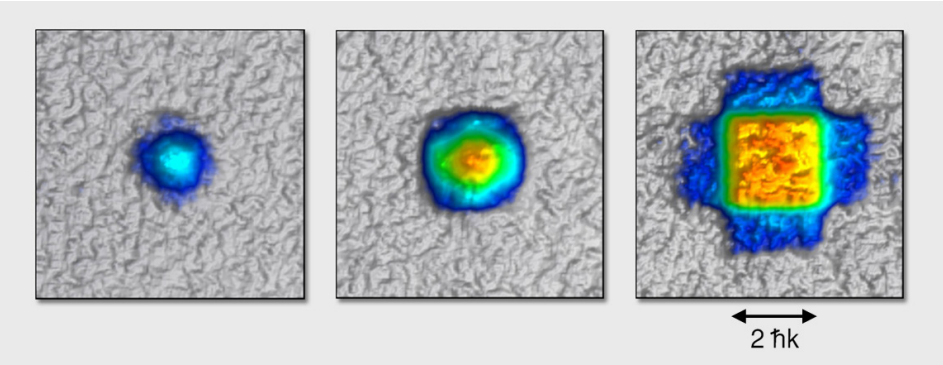

Test model: 3D Hubbard

$$H = -\sum_{\langle ij\rangle,\sigma} t_{ij}(c^{\dagger}_{i\sigma}c_{j\sigma} + c^{\dagger}_{j\sigma}c_{i\sigma}) + U\sum_{i} n_{i\uparrow}n_{i\downarrow}.$$

Temperatures in experiment are high (far above AFM phase).

Can we emulate the optical lattice emulator?
Numerically exact results needed!

Phys. Rev. Lett. 106, 030401 (2011)
Phys. Rev. B 83, 075122 (2011)

Controlling DCA (3d Hubbard, high T)

Solve quantum impurity model self-consistently for a range of cluster sizes:

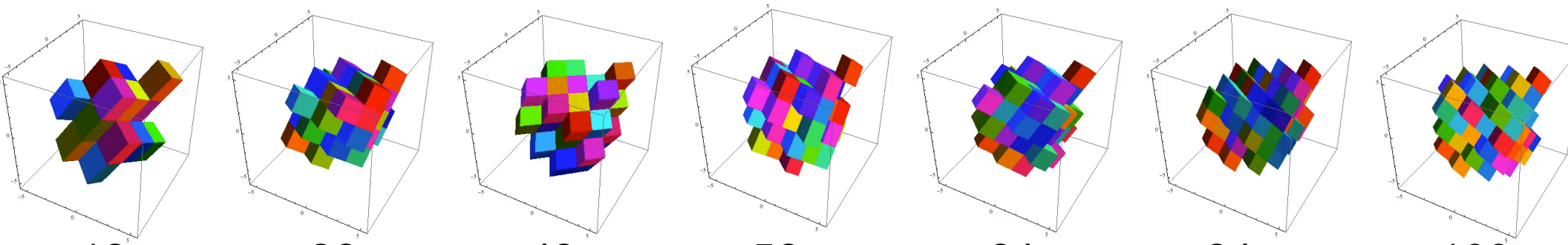

Compute thermodynamics: energy, density, entropy, free energy, double occupancy, spin correlation functions, …: Observable estimates and errors for a finite size system.

Extrapolate observable estimate to the infinite system size limit using known finite size scaling

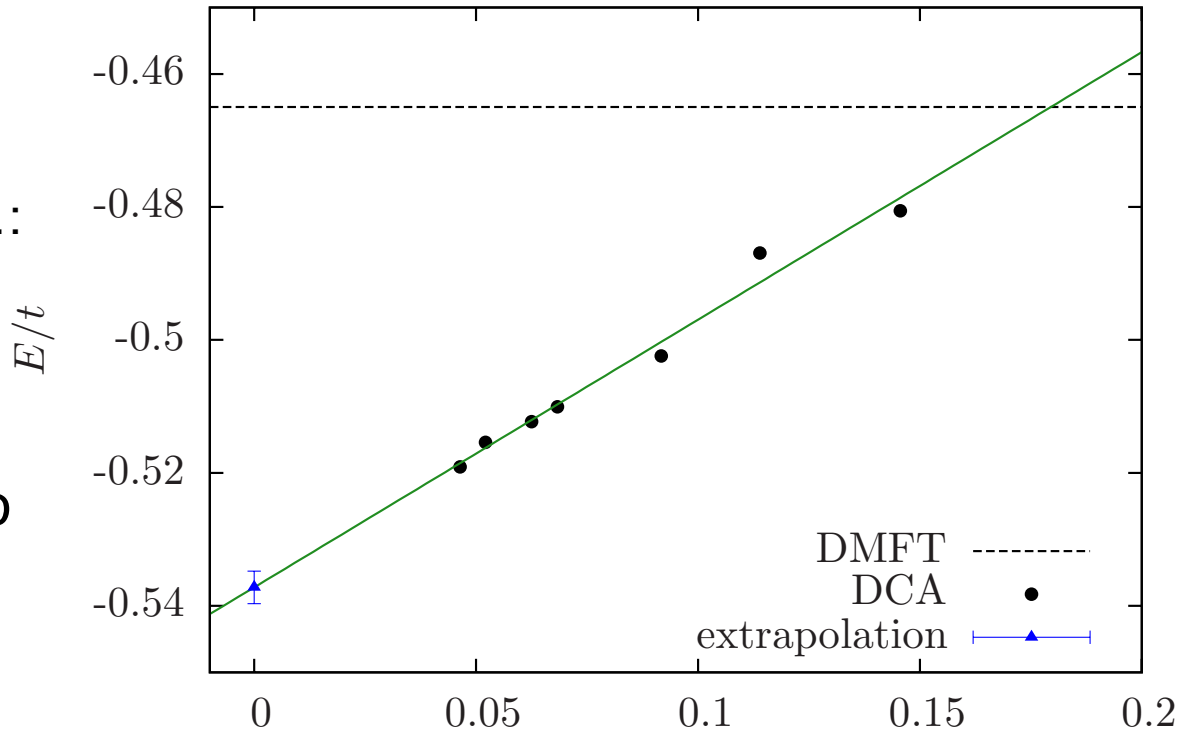

Fine size scaling behavior: Maier, Jarrell, Phys. Rev. B 65, 041104(R) (2002)

Phys. Rev. Lett. 106, 030401 (2011)

Controlling DCA (3d Hubbard, high T)

Validation against lattice QMC (1/2 filling) and HTSE (high T)

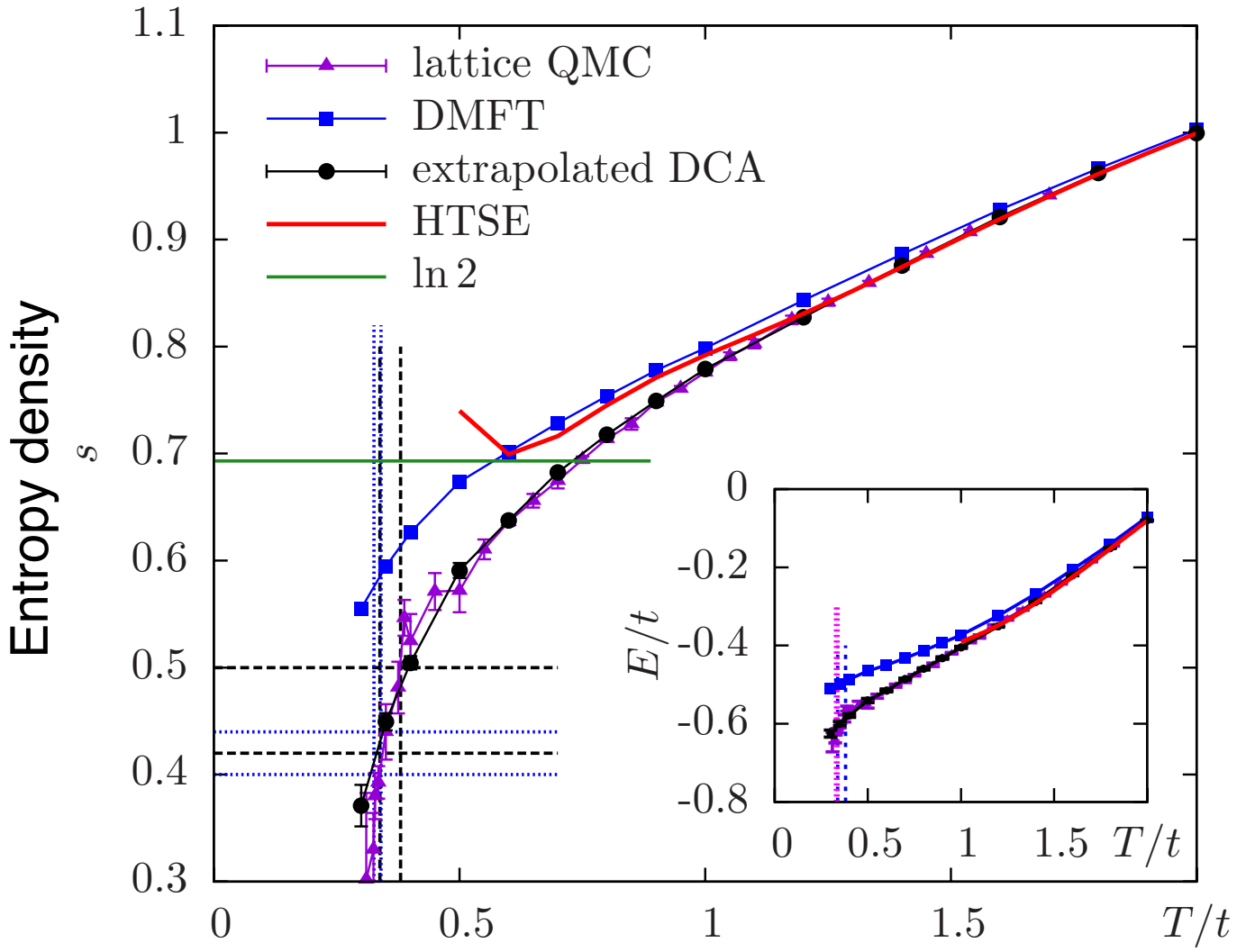

Phys. Rev. Lett. 106, 030401 (2011)

Controlling DCA (3d Hubbard, high T)

k-dependence of the self energy systematically reintroduced, convergence for self energy observed: Approximation controlled

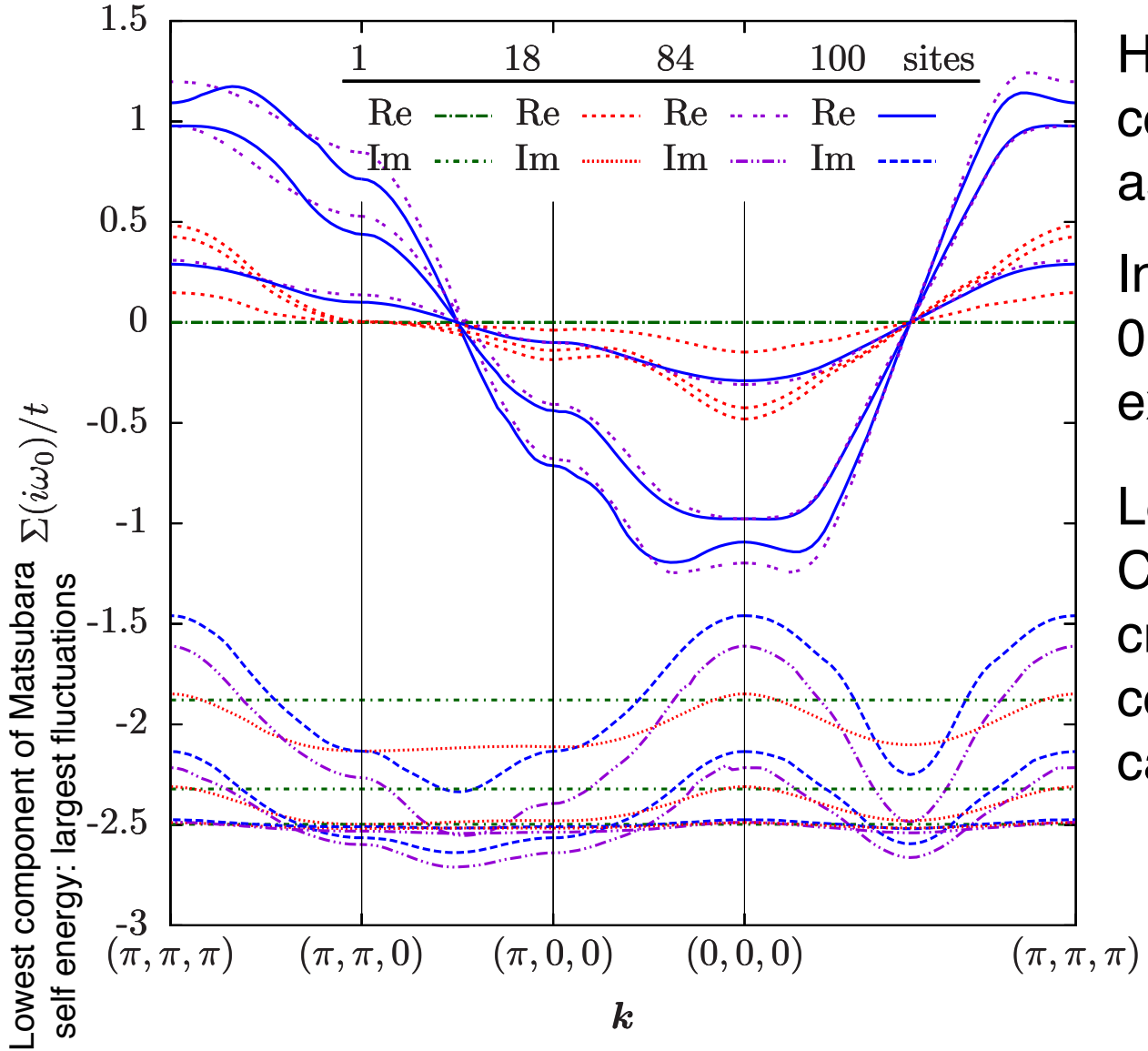

High temperature T/t = 1: Exact convergence of the self energy as a function of cluster size.

Intermediate temperature T/t = 0.5: Convergence visible, extrapolation needed.

Low temperature T/t = 0.35: Convergence not obvious, critical regime with diverging correlation length not well captured. (~T_N)

J. Le Blanc and E. Gull, Phys. Rev. B 88, 155108

2d High-T: extrapolations & exact results

Results from a series of clusters with typical cluster sizes: 50-100

Quantitative, numerically exact, stringent comparisons to other methods (linked cluster [very high T], lattice QMC [1/2 filling])

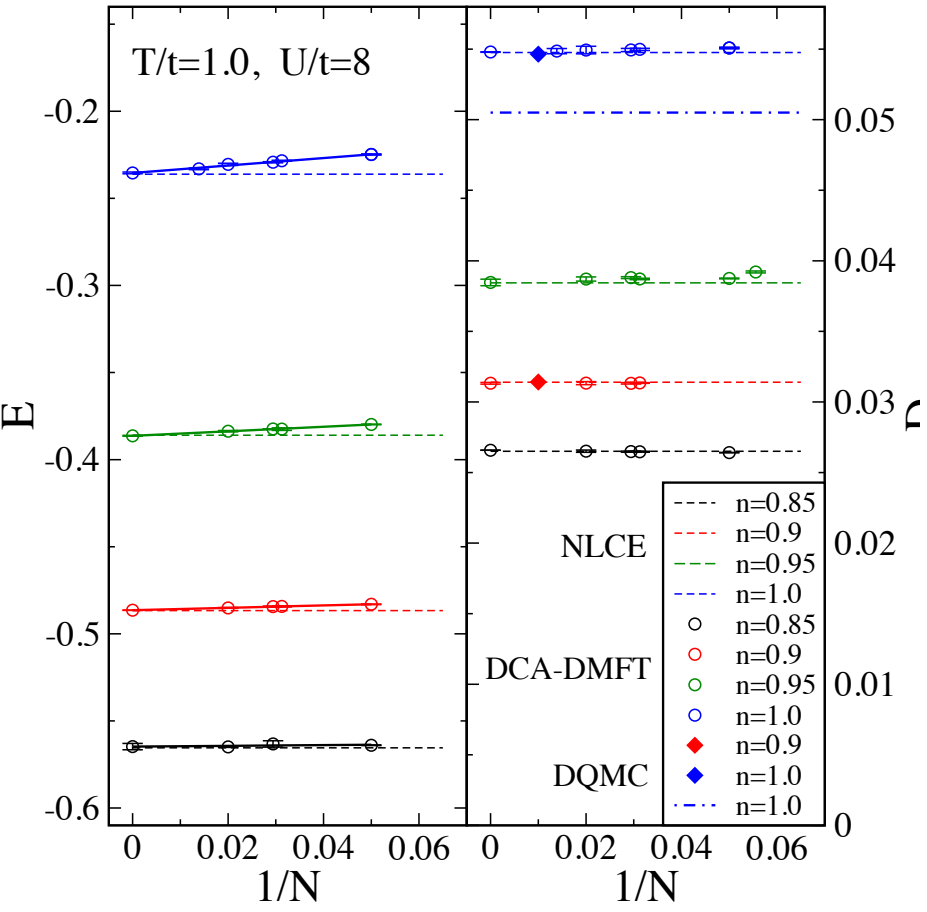

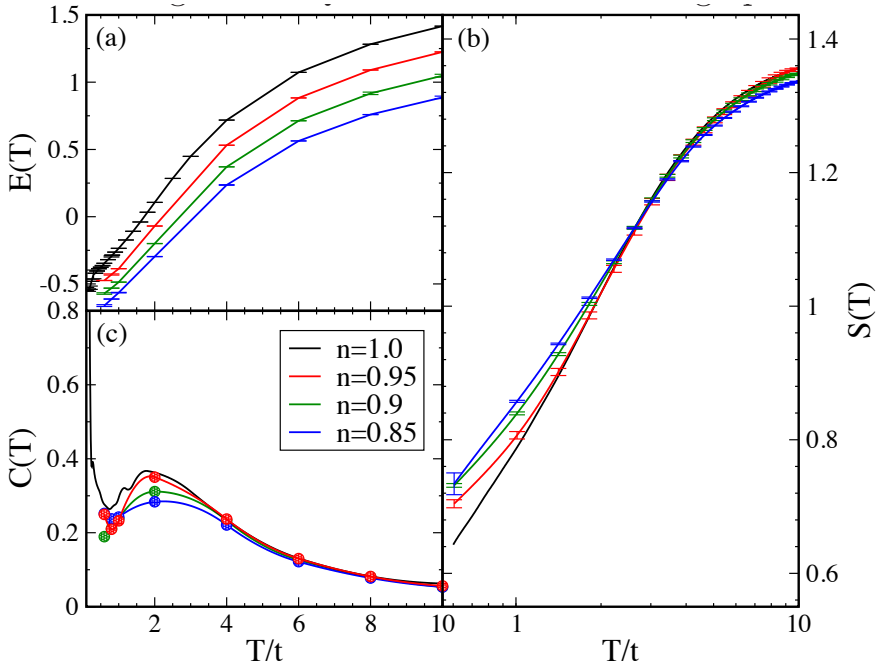

FIG. 6. (Color online) Energy, $E(T)$, entropy, $S(T)$, and specific heat capacity, $C(T)$, as functions of T/t extrapolated to the TL for $U/t = 8$ for filling values of $n = 0.85$, 0.9, 0.95, and 1.0 (half-filled).

E. Gull, P. Staar, S. Fuchs, et al., Phys. Rev. B 83, 075122 (2011)

Low-T: fermionic sign problem

For 2D at physically interesting interaction strengths and temperatures: **No quantitative extrapolation** to TD limit.

Variation of cluster sizes and geometries, establish robustness of results and trends. What is **artifact**, what is **general**?

For superconductivity: cluster geometries of size 4–16.

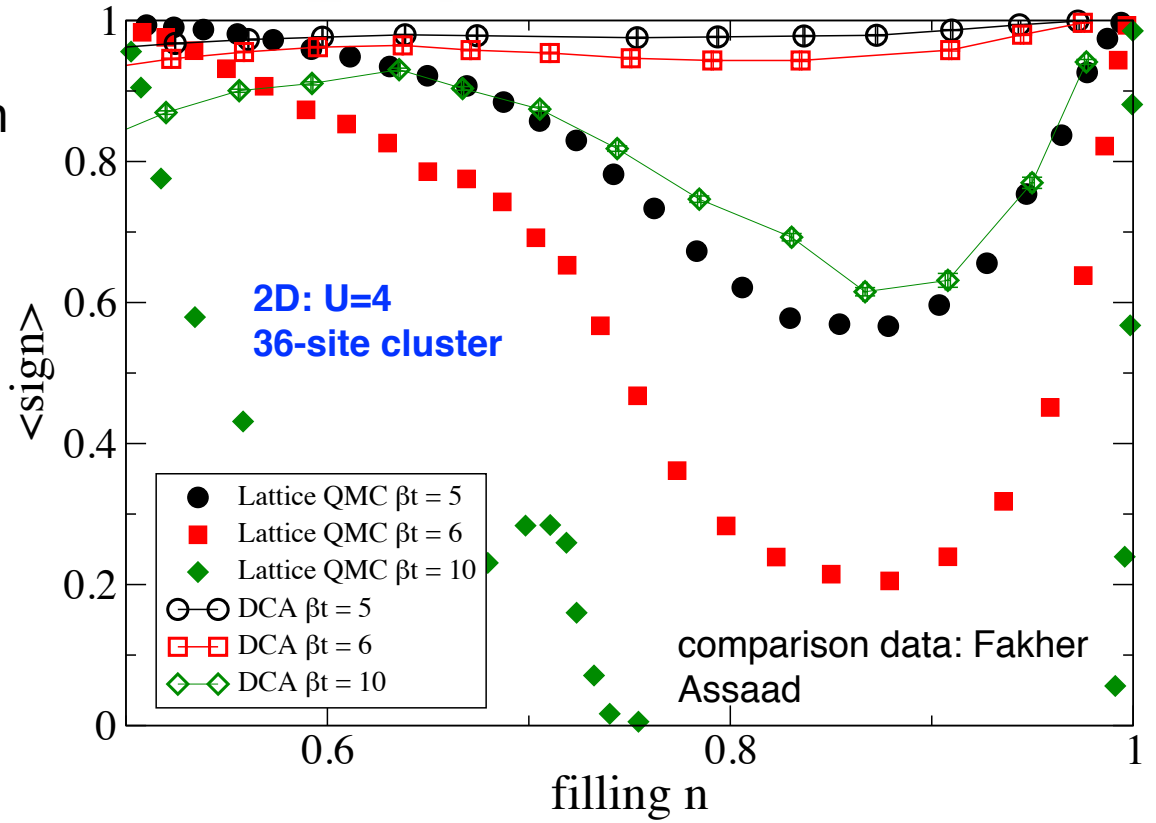

In practice: **only** hard limitation given by **fermionic sign problem** of QMC solver

Dynamical mean field bath helps to increase <sign>, convergence to TD limit becomes more regular, absence of shell effects.

Approximation to Sigma, not G.

MC possible to scale to 10'000s of compute cores (ALPS libraries)

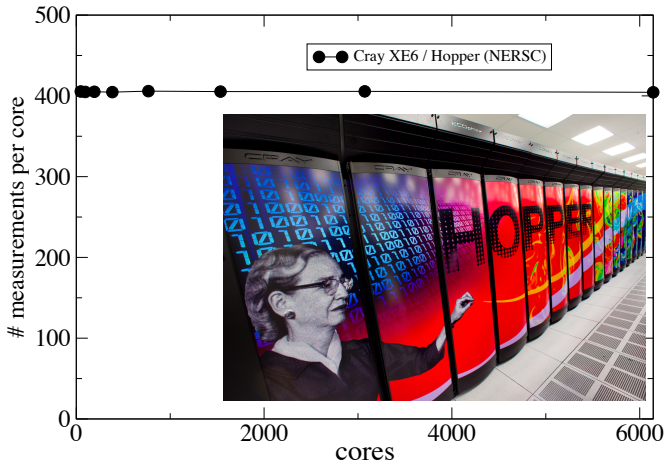

Emanuel Gull and Andrew J. Millis, arXiv:1407.0704

Generic U/doping Phase Diagram (high T, no t', disordered phase, ~ 200K)

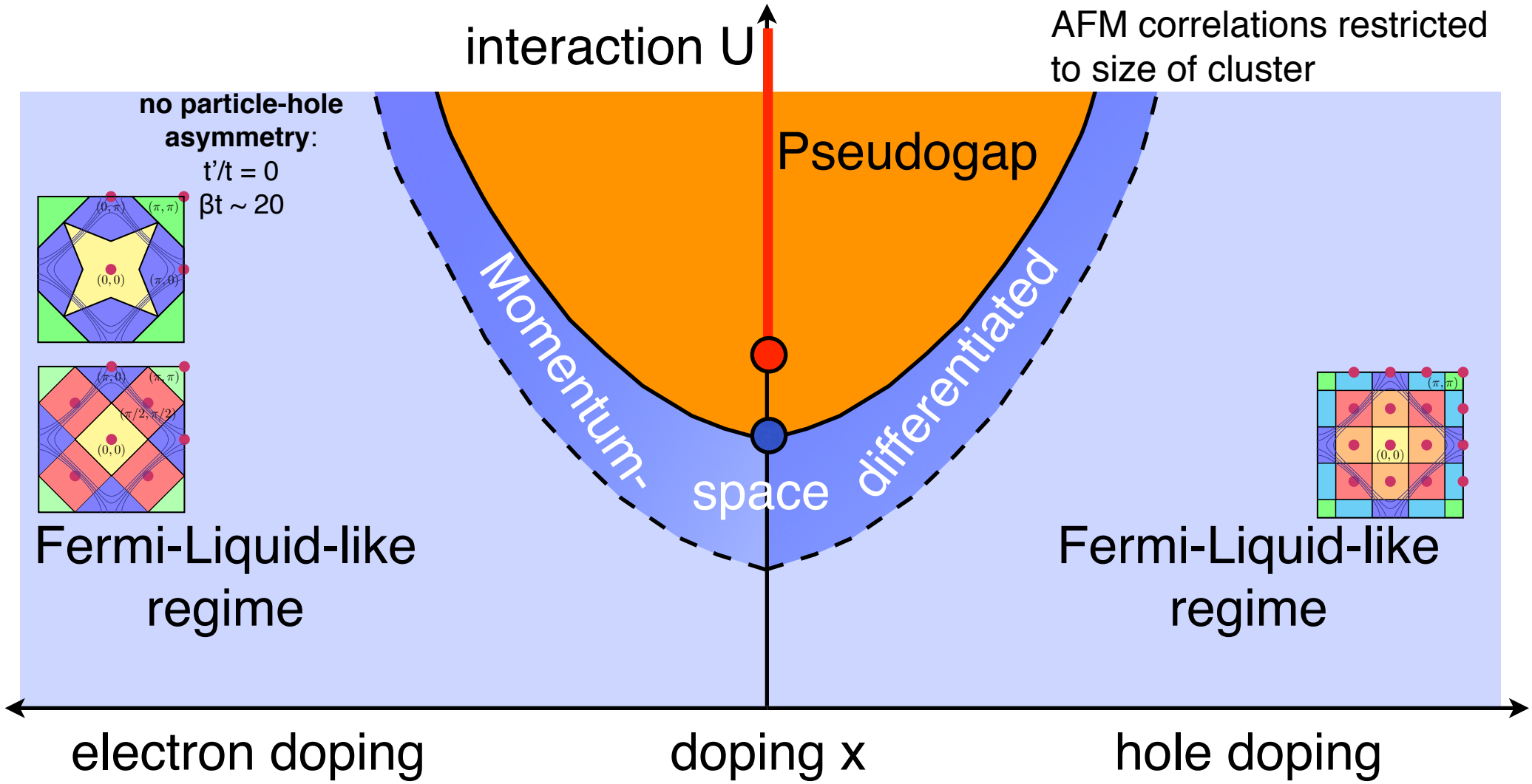

P. Werner, E. Gull, O. Parcollet, A. J. Millis, Phys. Rev. B 80, 045120 (2009) (interaction)
E. Gull, O. Parcollet, P. Werner, A. J. Millis, Phys. Rev. B 80, 245102 (2009) (doping, t')
E. Gull, M. Ferrero, O. Parcollet, A. Georges, A.J. Millis, Phys. Rev. B 82, 155101 (2010) (cluster size)

Emanuel Gull and Andrew J. Millis, arXiv:1407.0704

Generic U/doping Phase Diagram (high T, t', disordered phase, ~ 200K)

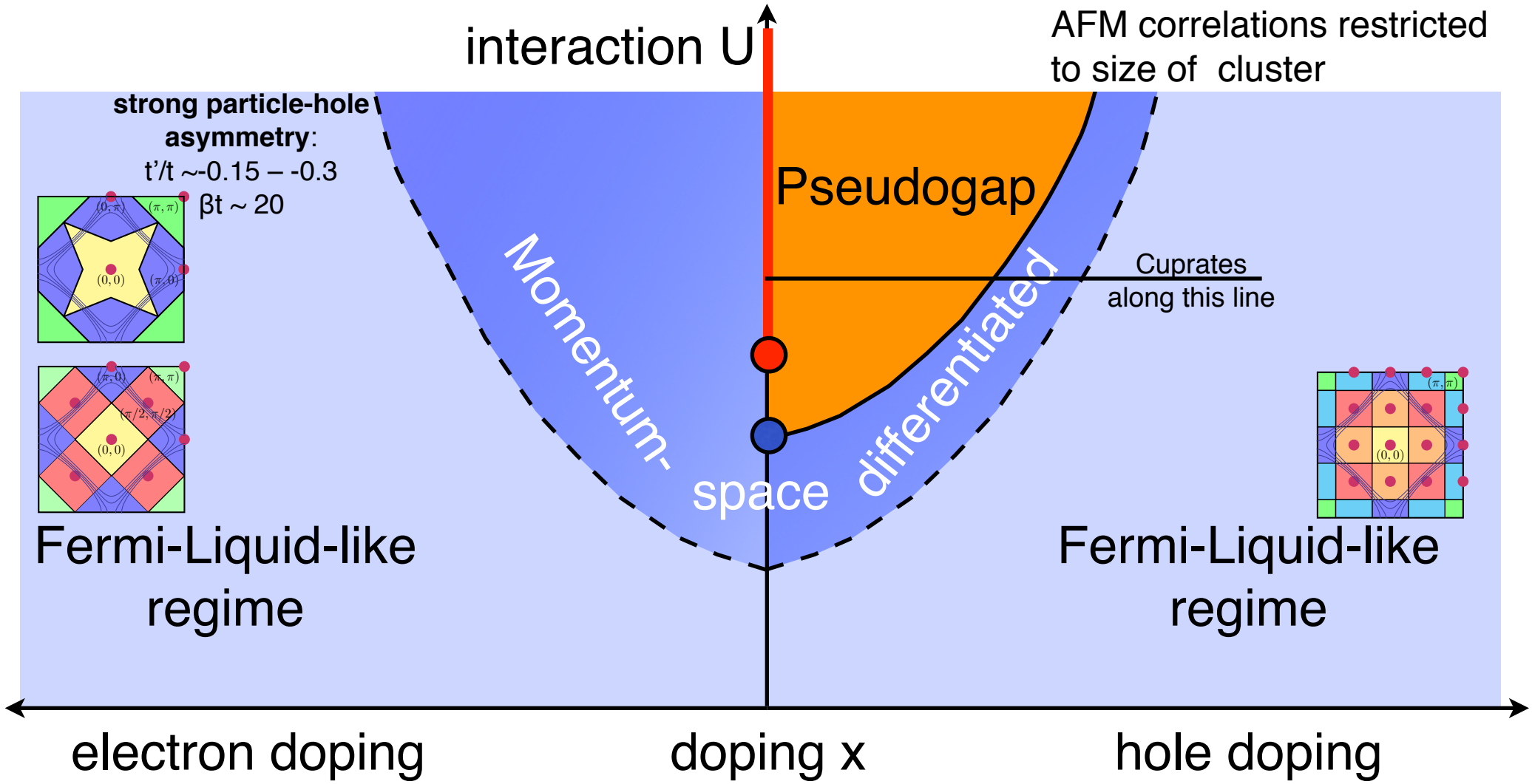

E. Gull, O. Parcollet, P. Werner, A. J. Millis, Phys. Rev. B 80, 245102 (2009) (doping, t')
P. Werner, E. Gull, O. Parcollet, A. J. Millis, Phys. Rev. B 80, 045120 (2009) (interaction)
E. Gull, M. Ferrero, O. Parcollet, A. Georges, A.J. Millis, Phys. Rev. B 82, 155101 (2010) (cluster size)

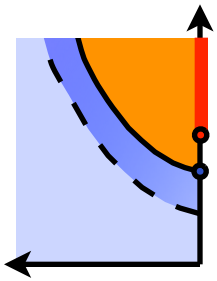

N. Lin, E. Gull, and A.J. Millis, Phys. Rev. B 82, 045104 (2010)

Pseudogap Regime: Spectra

Analytically continued* spectral function A(ω): U = 7t, t'/t=0.15, βt=20
(for various dopings, as a function of frequency)

for the antinodal region

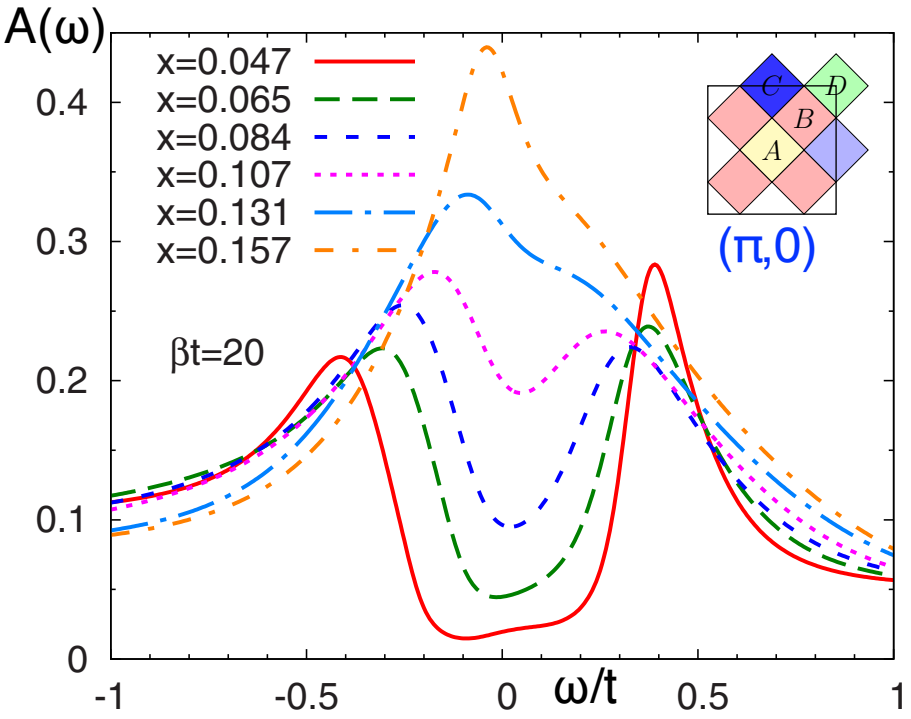

for the nodal region.

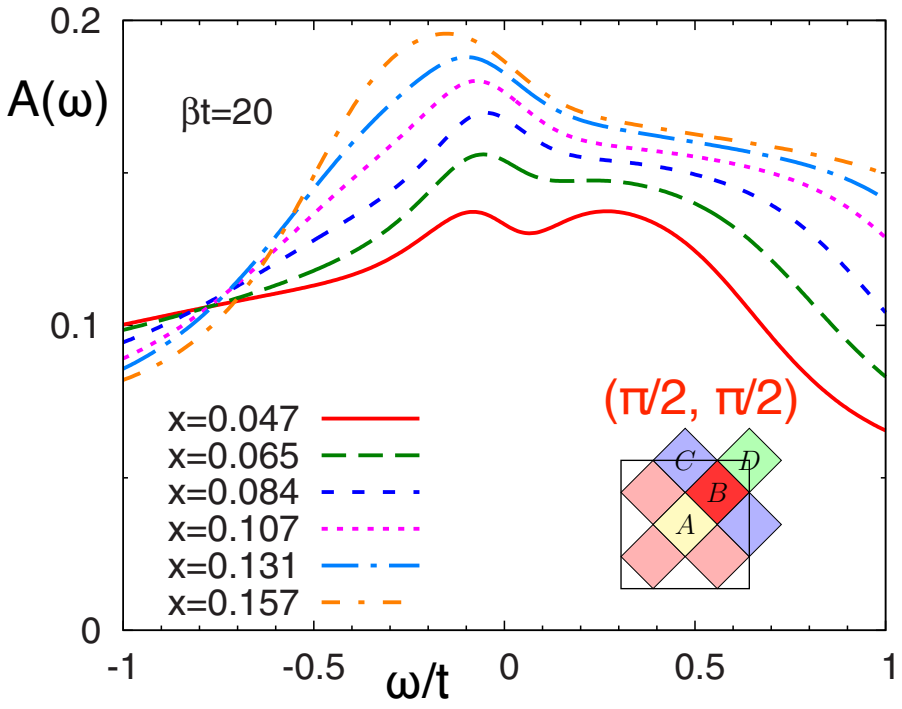

when reducing doping from x=0.157 to x=0.047: gap develops in the antinodal part of BZ, nodal part stays metallic.

*Maximum entropy of self-energy data

See also talk by A.-M. Tremblay

d-wave Superconductivity

Low enough temperature to access the superconducting phase

- **Large clusters that have a clear pseudogap state, different geometries**!

- **Interactions strong enough** that half-filled system is Mott insulating

- **Numerically exact algorithms** (no bath fitting, no imaginary time discretization)

- Increase of CPU power makes **surveys of phase space** possible

- Precision good enough to perform reliable analytic continuation

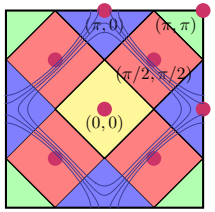

d-wave superconductivity:
anomalous antinodal self-energy
(- - - -) at (pi,0) and **(- - - -)** at (0,pi)

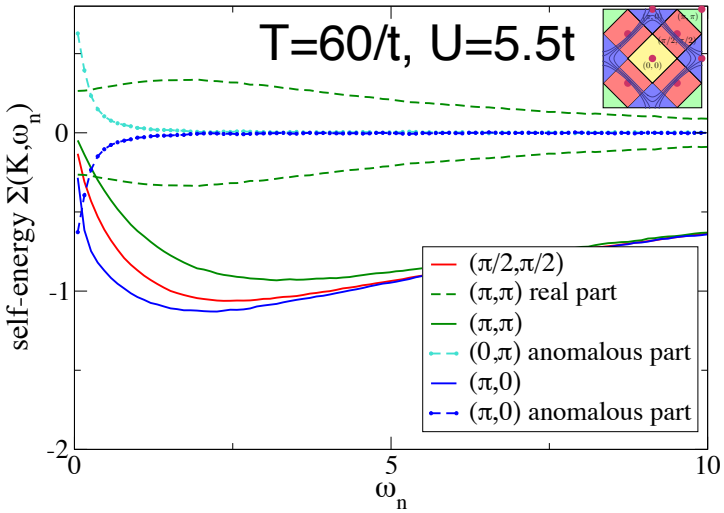

Previous work: Large clusters, phase boundary from normal state susceptibilities, U/t=4: **Maier, Jarrell**, et al., Phys. Rev. Lett. 95, 237001 (2005)

4-site clusters (Hirsch Fye), formalism: **Lichtenstein, Katsnelson**: Phys. Rev. B 62, R9283 (2000), NCA: **Maier, Jarrell, Pruschke, Keller**, Phys. Rev. Lett. . 85, 1524–1527 (2000), ED: **Kancharla** et al, PRB '08, **Civelli** et al, PRL 08,09, PRB 08, CT-HYB: **Sordi** et al., PRL 2010 / 2012.

E. Gull, O. Parcollet, A.J. Millis, Phys. Rev. Lett. 110, 216405 (2013)

Generic U/doping Phase Diagram (low T, superconducting phase, ~ 100K)

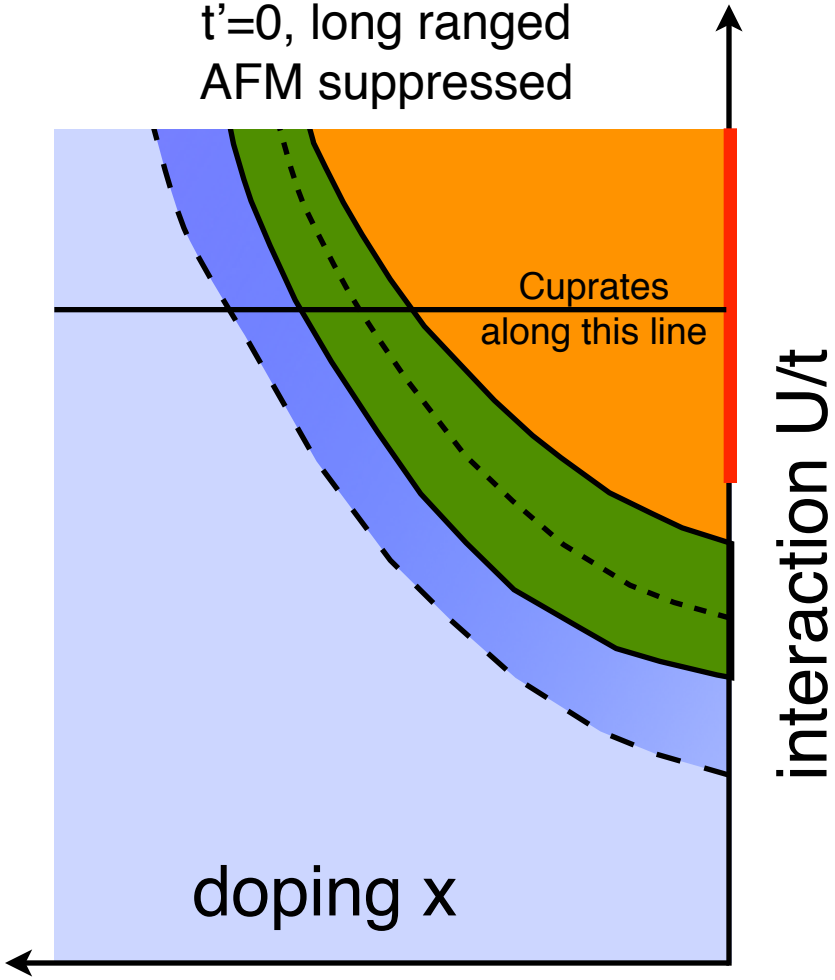

Additional low-T phase:

- d-wave superconductivity
- Mott Insulator
- Non-superconducting pseudogap regime
- Momentum-space differentiated regime [no sc]
- Non-superconducting Fermi-Liquid-like regime

On clusters large enough to allow for nodal/antinodal differentiation:

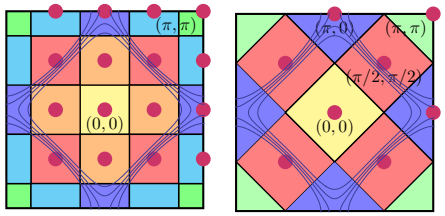

E. Gull, O. Parcollet, A.J. Millis, Phys. Rev. Lett. 110, 216405 (2013)

Phase Diagram (T/t = 1/60)

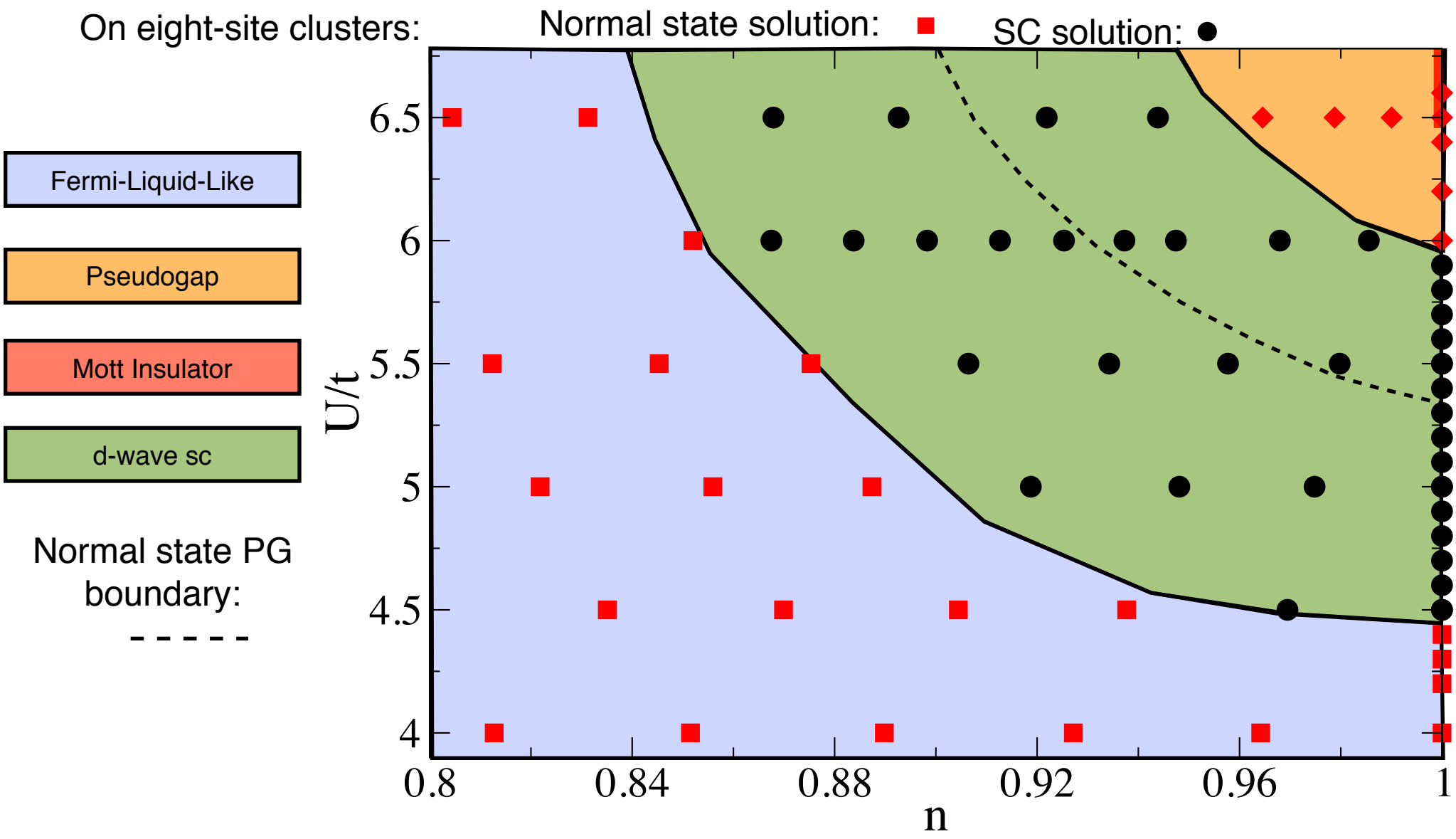

E. Gull, A.J. Millis, Phys. Rev. B 86, 241106(R) (2012)

Energy differences (doping)

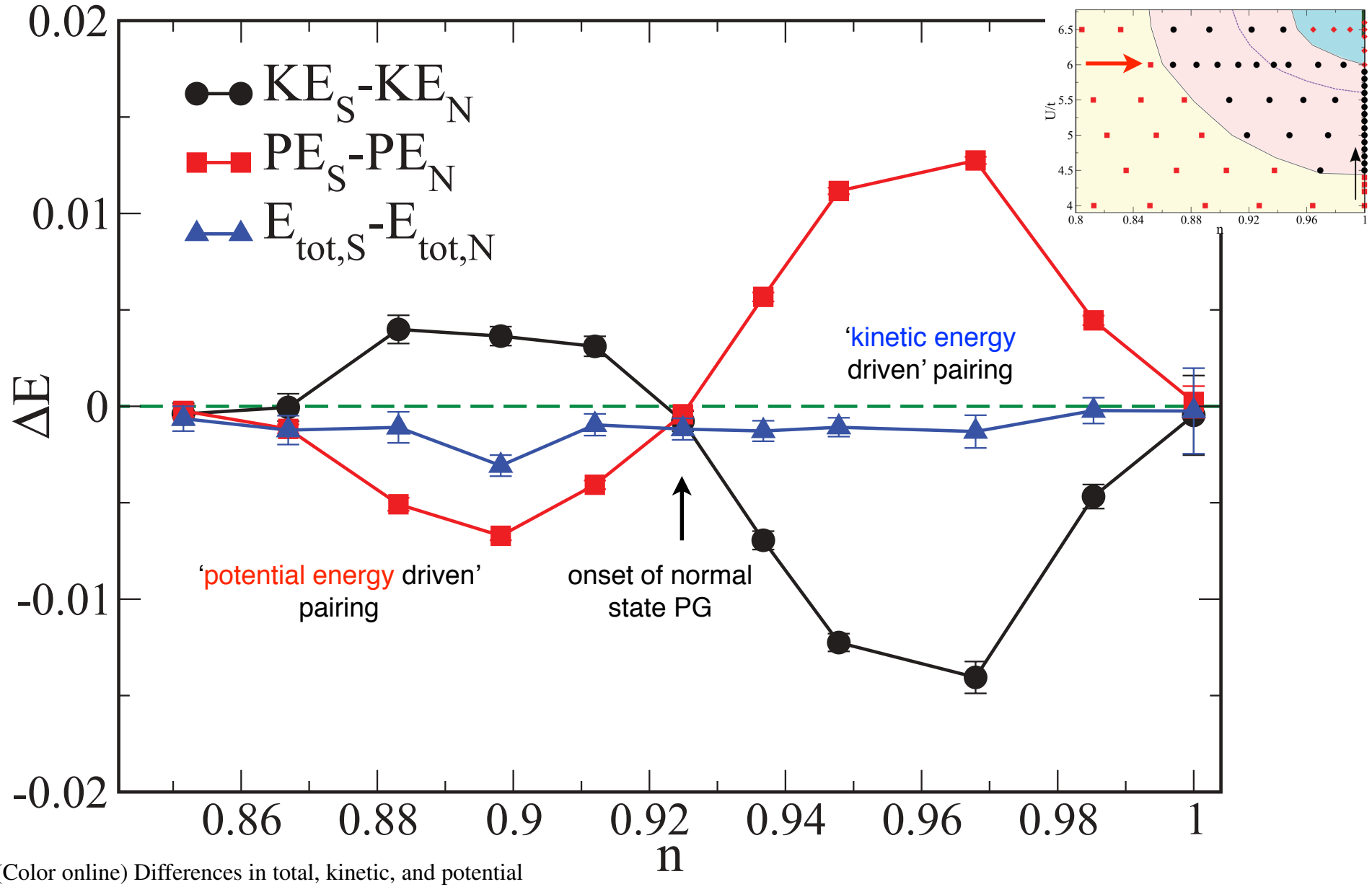

FIG. 2. (Color online) Differences in total, kinetic, and potential energies (per site, in units of hopping t) between normal and superconducting states, obtained as described in the text at density $n = 1$ varying interaction strength (upper panel) and as function of density at fixed interaction strength $U = 6t$ (lower panel).

E. Gull, O. Parcollet, A.J. Millis, Phys. Rev. Lett. 110, 216405 (2013)

Superconducting spectral function overdoped / optimally doped region

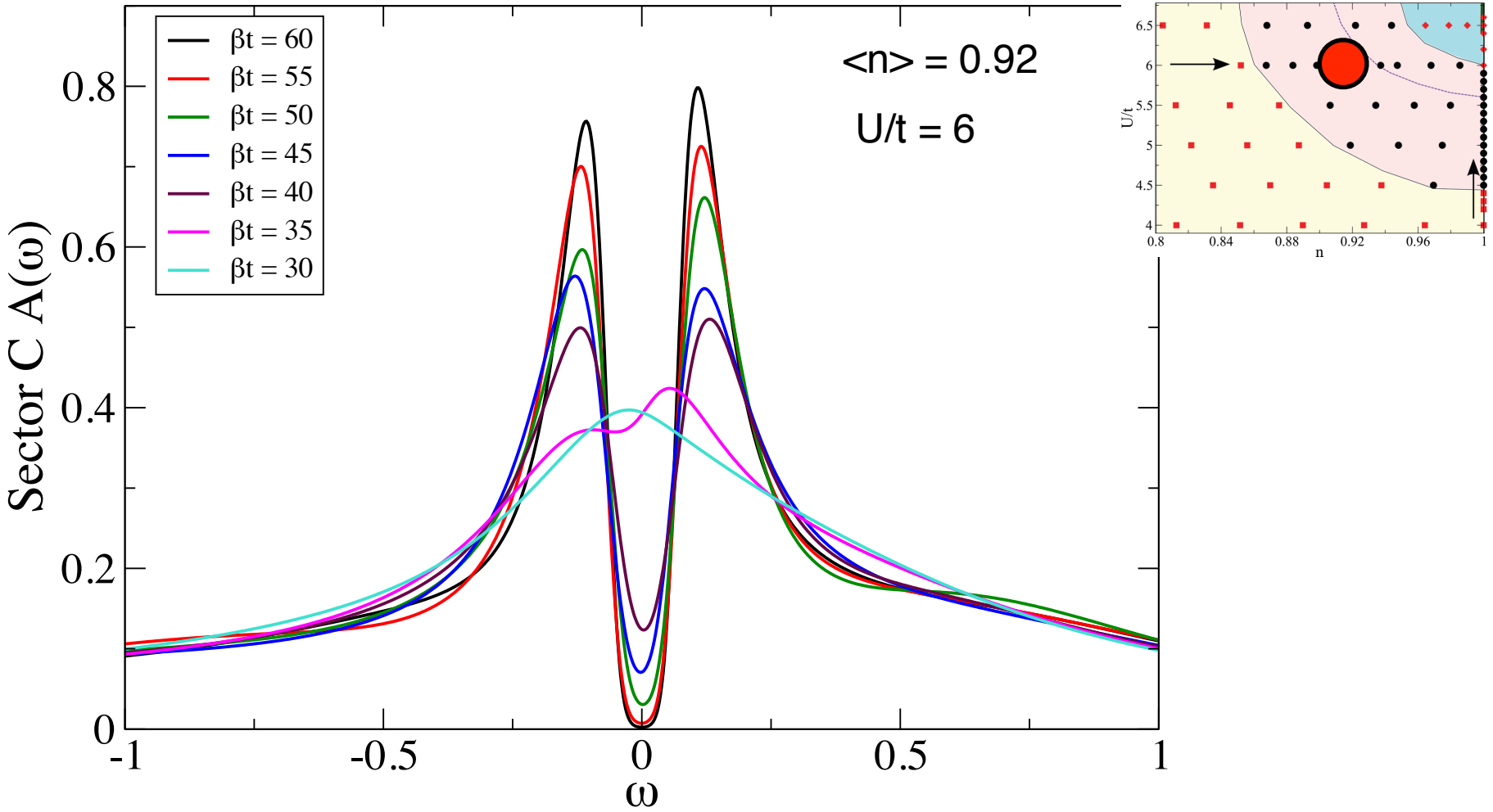

- symmetric spectral function, quasiparticle peaks on both sides. Weight in peaks from vicinity of Fermi energy

- superconducting gap at the antinode

E. Gull, O. Parcollet, A.J. Millis, Phys. Rev. Lett. 110, 216405 (2013)

Superconducting spectral function: underdoped region

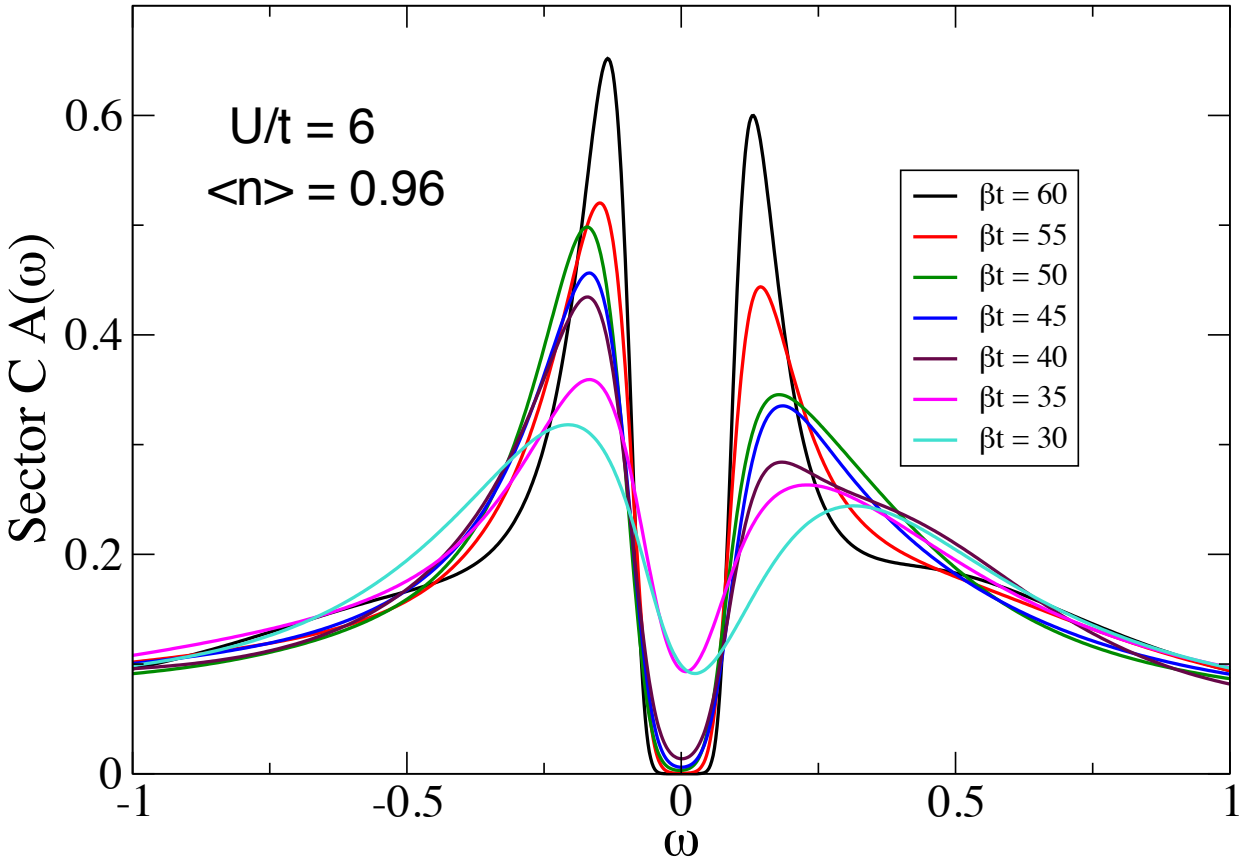

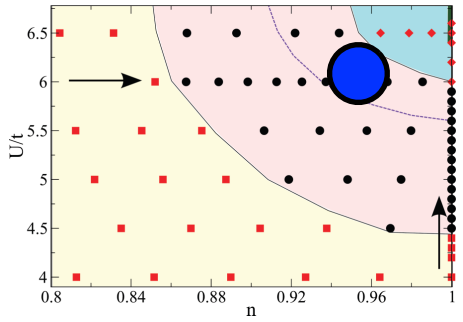

Pseudogap state at high T very different from SC state at low T: fundamental rearrangement of spectral weight on energy scales $\gg \Delta$. Superconducting gap significantly smaller than pseudogap. (conclusion independent of continuation)

E. Gull, A.J. Millis, Phys. Rev. B 86, 241106(R) (2012)

Response to applied field

small response to sc field in pseudogap regime shows that PG and superconductivity are **in competition**

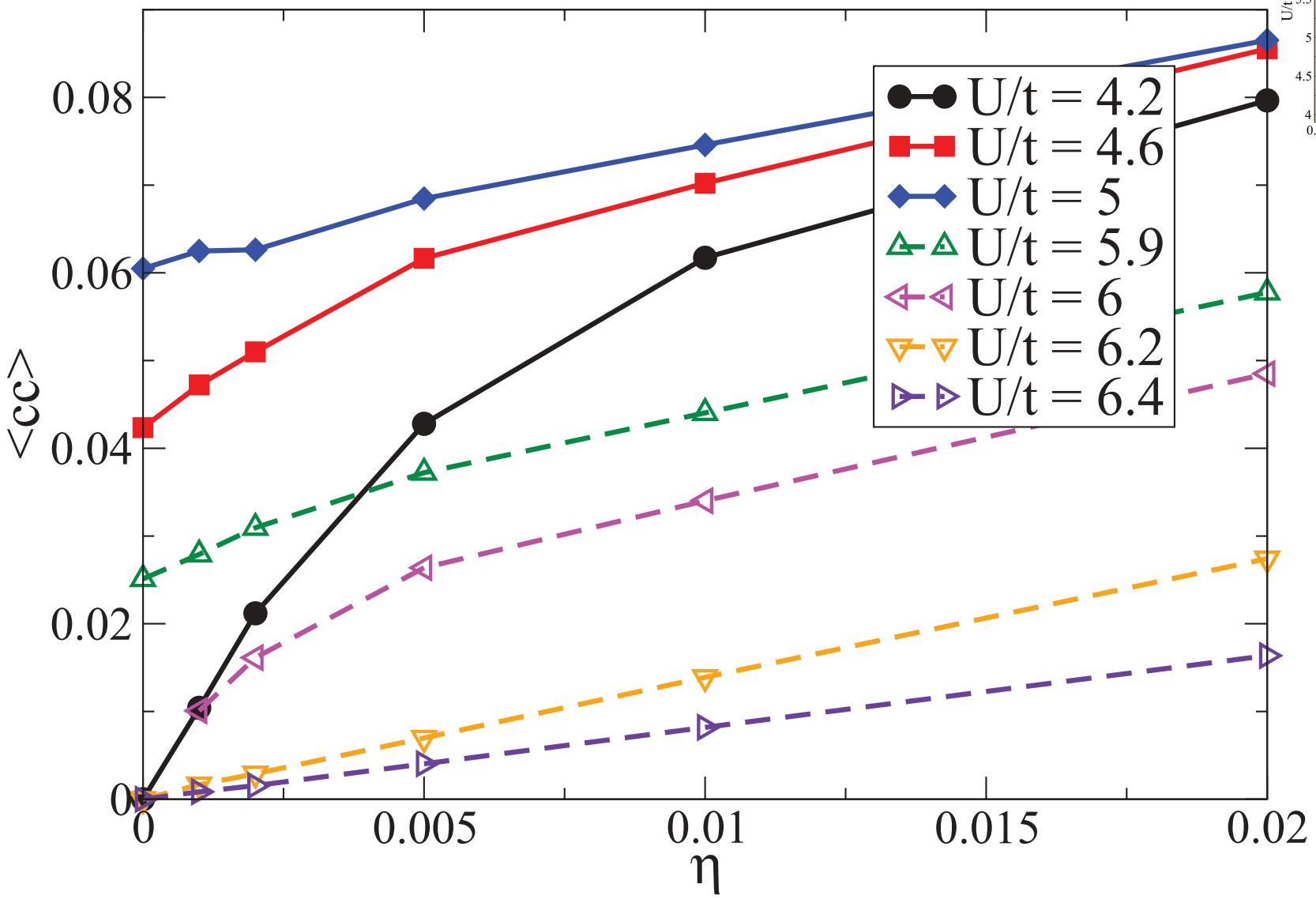

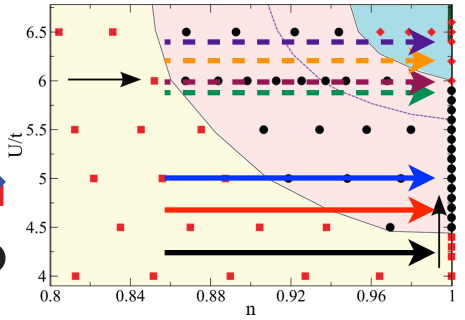

FIG. 3. (Color online) Anomalous expectation value in sector $K = (0,\pi)$ plotted against pairing field η at doping $x = 0$ for interaction strengths indicated.

Emanuel Gull and Andrew J. Millis, arXiv:1407.0704

Analytic continuation of self-energy

- Matsubara self-energy:

$$\mathbf{\Sigma}(k, i\omega_n) = \begin{pmatrix} \Sigma^N(k, i\omega_n) & \Sigma^A(k, i\omega_n) \\ \Sigma^A(k, i\omega_n) & -\Sigma^N(k, -i\omega_n) \end{pmatrix}$$

- Real frequency self-energy:

$$\Sigma^{N,A}(z) = \int \frac{dx}{\pi} \frac{\mathrm{Im}\Sigma^{N,A}(x)}{z - x}.$$

- Inversion of this kernel is ill conditioned, noise in data is amplified. Perform ‘maximum entropy’ procedure.

Jarrell, Gubernatis, Physics Reports 3, 133 (1996)

- Maximum entropy requires Im Sigma to be of the same sign for all frequencies. OK for normal components.

Wang *et al.*, Phys. Rev. B 80, 045101 (2009)

Emanuel Gull and Andrew J. Millis, arXiv:1407.0704

Analytic continuation of self energies

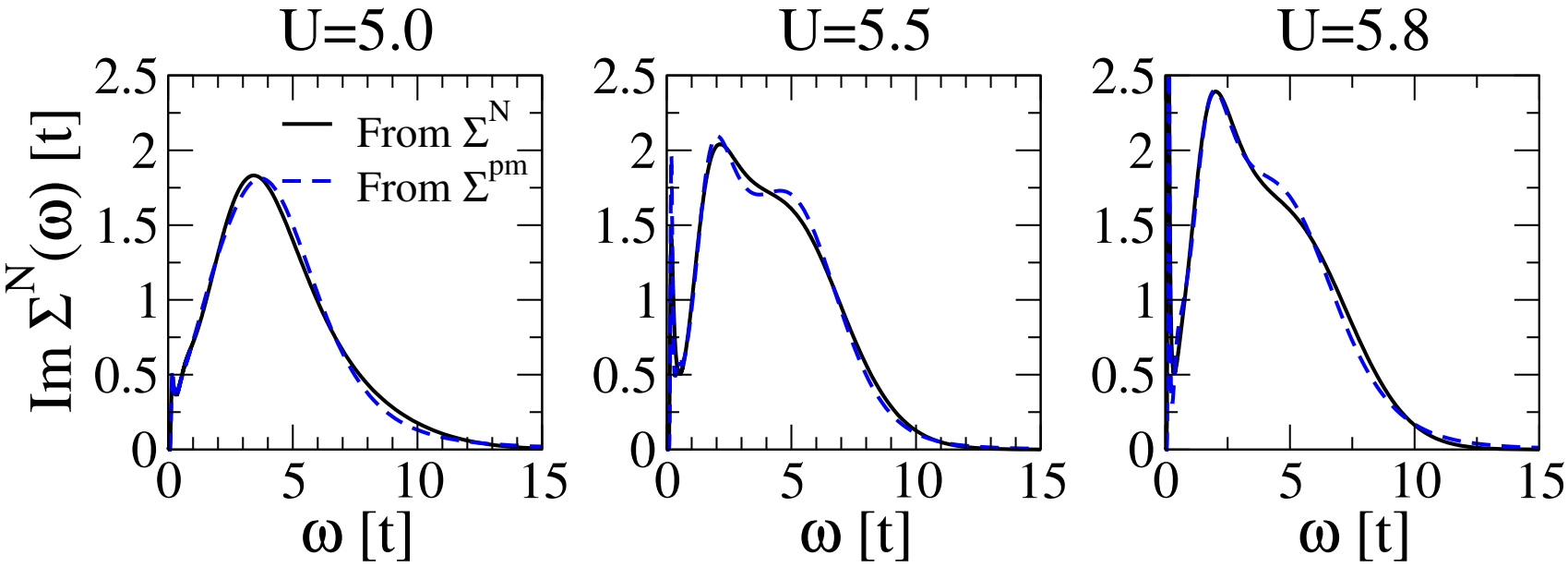

- Analytic continuation of normal part of superconducting antinodal self-energy for different interactions at half-filling (metastable superconducting state).

- U=5: 'weak coupling' state
- U=5.8: pseudogap state

- Different methods of analytic continuation (same input data) described by different line shapes.

- Normal part of self-energy shows narrow peak at low energy & broad higher frequency maximum

Emanuel Gull and Andrew J. Millis, arXiv:1407.0704

Analytic continuation of self-energy

$$\Sigma^{N,A}(z) = \int \frac{dx}{\pi} \frac{\mathrm{Im}\Sigma^{N,A}(x)}{z-x}.$$

- Anomalous self-energy is an odd function of frequency: not a positive function – no maxent possible

$$\Sigma^{A}(i\omega_n) = \int \frac{dx}{\pi} \frac{x}{i\omega_n - x} \left(\frac{\mathrm{Im}\Sigma^{A}(x)}{x} \right)$$

- Modified continuation kernel takes into account odd frequency of anomalous self energy. Still no guarantee for positivity of $\mathrm{Im}\Sigma^{A}(\omega)/\omega$

- Basis transform to a plus/minus basis guarantees positivity for the half-filled case

$$c^{\pm}_{k\sigma} = \left(c^{\dagger}_{k\sigma} \pm c_{-k,-\sigma} \right) / \sqrt{2} \qquad \mathbf{G}^{\pm} = \begin{pmatrix} \mathcal{G}_0^{-1}(z) - \Sigma^{+}(z) & 0 \\ 0 & \mathcal{G}_0^{-1}(z) - \Sigma^{-}(z) \end{pmatrix}^{-1}$$

- Maxent possible for half filled case. Away from half filling: negative features in +/- basis in principle possible but not observed in Padé; Maxent consistent with positive $\mathrm{Im}\Sigma^{A}(\omega)/\omega$

Analytic continuation of self-energy

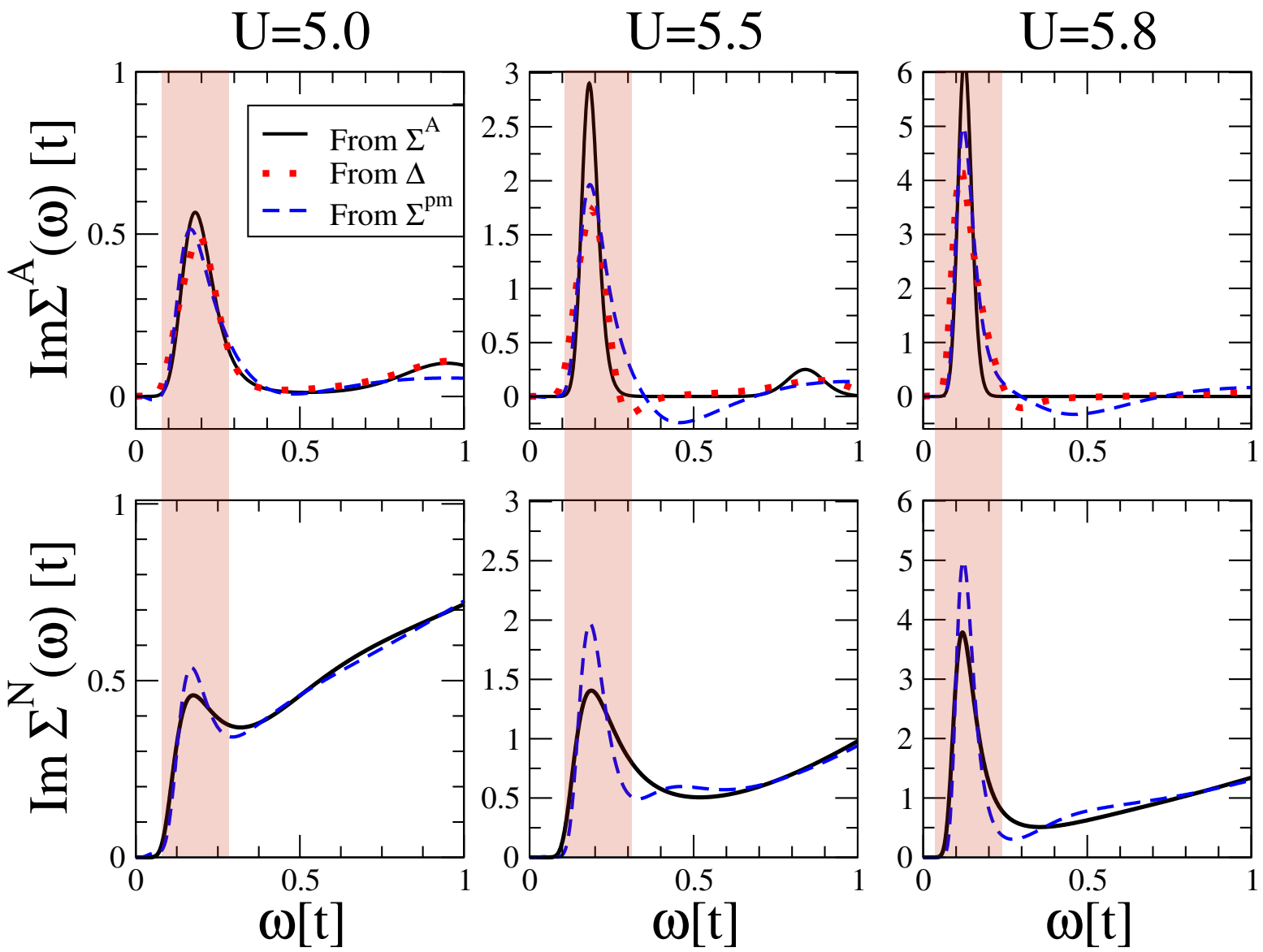

Anomalous component of superconducting self-energy

Normal component of superconducting self-energy

Three maxent procedures with different uncertainties. Half filled (metastable) case.
Peak at relatively low frequencies, followed by broad normal state features.
No negative component of anomalous self-energy found.

See also talk by A.-M. Tremblay, Civelli PRB '08, '09, PRL 09; PRB Kancharla et al. '08

Gap function

Green's function

$$G(k, i\omega_n) = \begin{pmatrix} i\omega_n - \epsilon_k - \Sigma^N(i\omega_n) & \Sigma^A(i\omega_n) \\ \Sigma^A(i\omega_n) & i\omega_n + \epsilon_k - \Sigma^N(-i\omega_n) \end{pmatrix}^{-1}$$

$$\det\left(G^{-1}\right) = -\left(1 - \frac{\Sigma_o^N(k,\omega_n)}{i\omega_n}\right) \times \left(\omega_n^2 + \left(\varepsilon^\star(k,\omega_n)\right)^2 + \Delta^2(k,\omega_n)\right)$$

$$\varepsilon^\star = \frac{\varepsilon_k + \Sigma_e^N(k,\omega_n)}{1 - \frac{\Sigma_o^N(k,\omega_n)}{i\omega_n}}$$

$$\Sigma_{o,e}^N = \frac{\Sigma^N(k,\omega_n) \mp \Sigma^N(k,-\omega_n)}{2}$$

Gap function

$$\Delta(k,\omega) = \frac{\Sigma^A(k,\omega)}{1 - \frac{\Sigma_o^N(k,\omega)}{\omega}}$$

Gap function

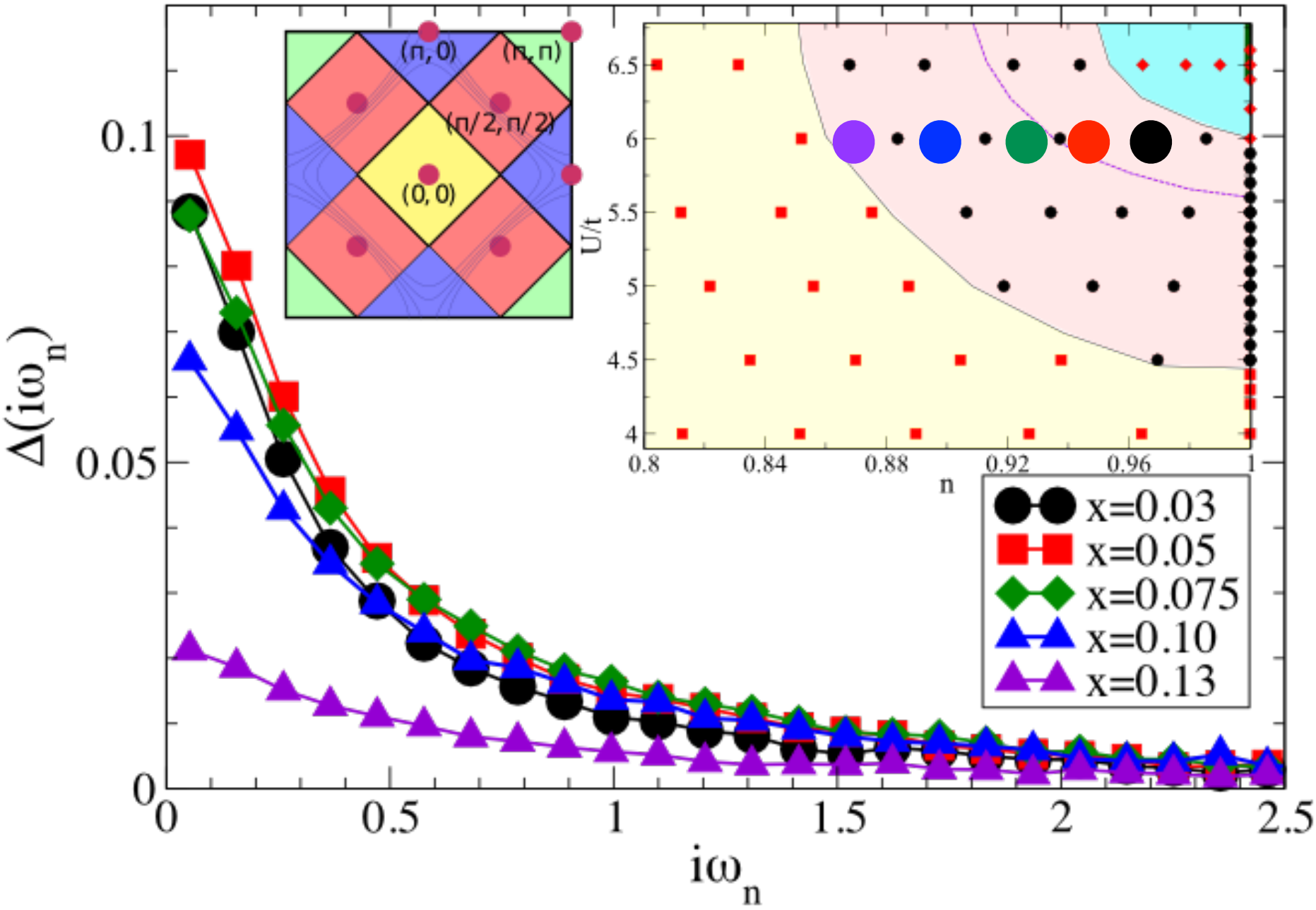

Gap function

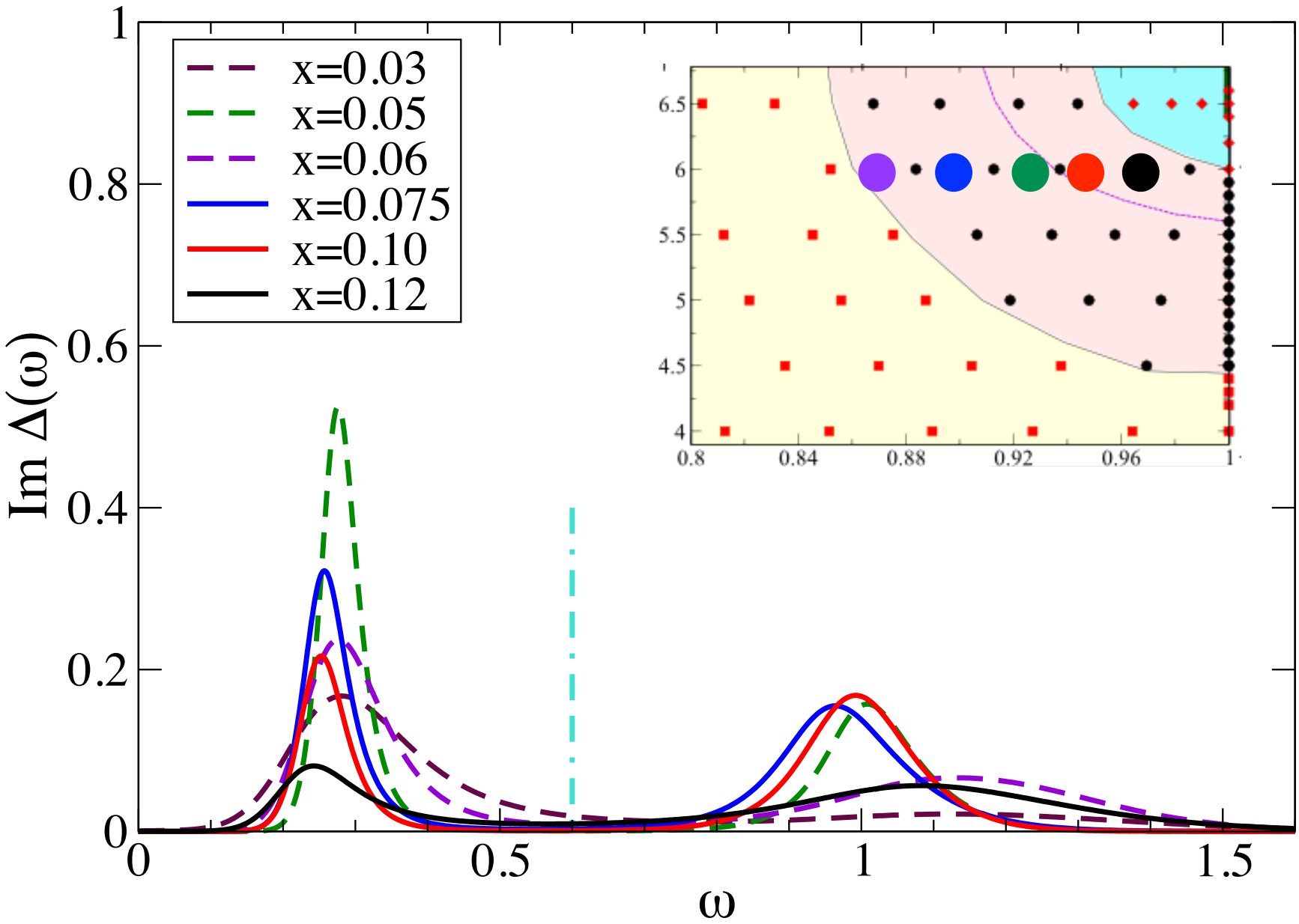

Comparison to experiment

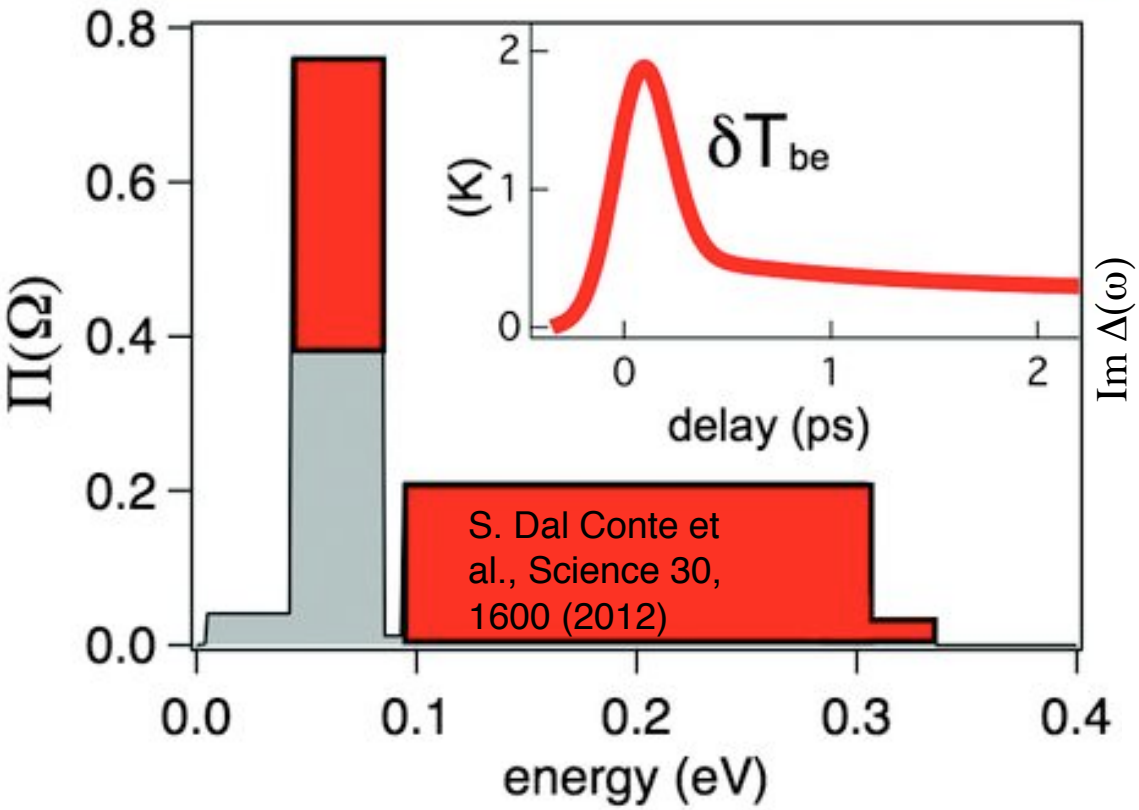

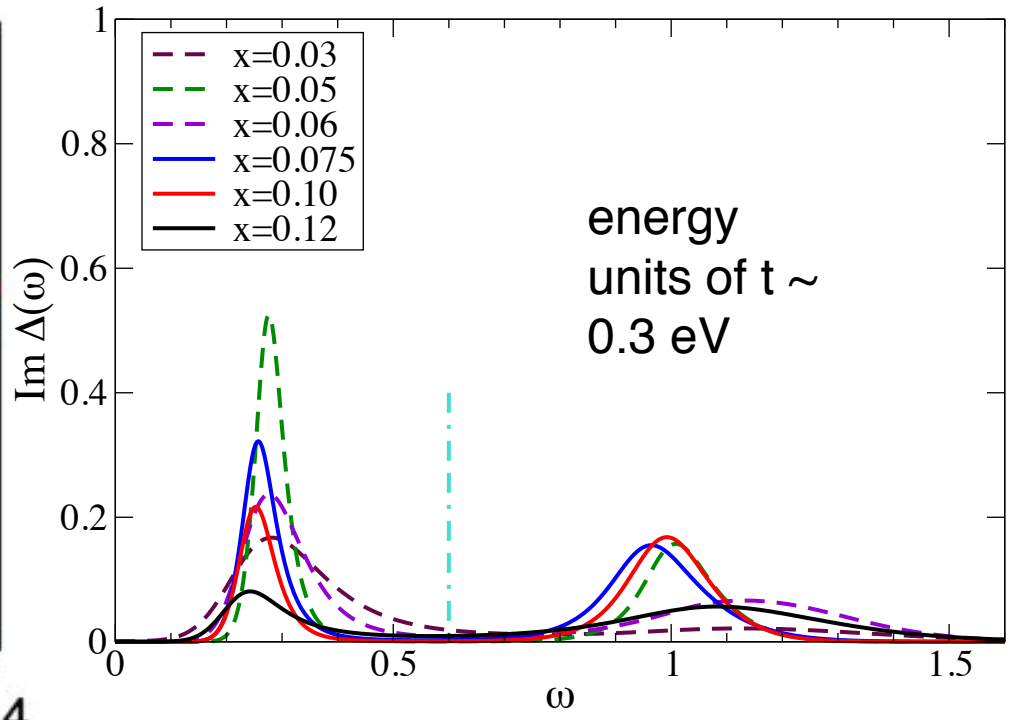

- S. Dal Conte et al., Science 30, 1600 (2012): Disentangling the Electronic and Phononic Glue in a High-Tc Superconductor:
- Measurement of different contributions to the gap function using nonequilibrium optical spectroscopy with femtosecond time resolution and ~10 meV energy resolution.
- Electronic contribution (red) to gap function.

Brief conclusion

Results from **cluster DMFT** (coarse grained self-energy) obtained on **8-site clusters**.

Simulations performed inside the **superconducting state** (Nambu formalism). Monte Carlo data analytically continued to real axis.

Anomalous self energy shows **structure only on low frequencies** (consistent with single peak)

Gap function shows structure at low frequencies (t ~ 0.25) up to t ~ 1, most of the weight concentrated at low frequencies.

Low frequency structure expected from **low-frequency collective excitations**, for example spin fluctuations.

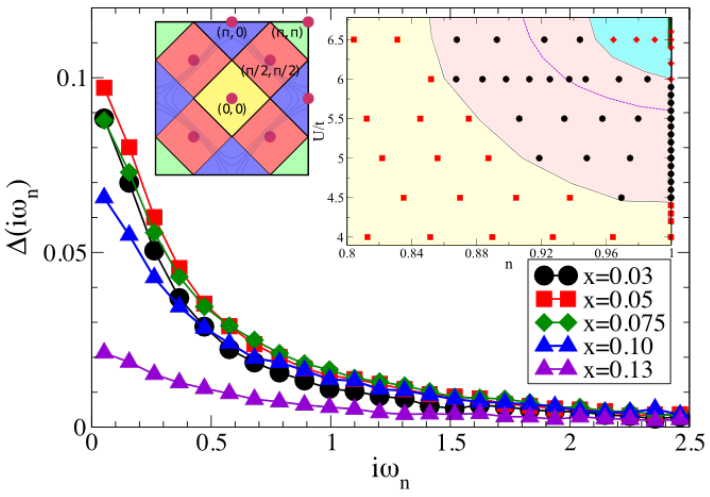

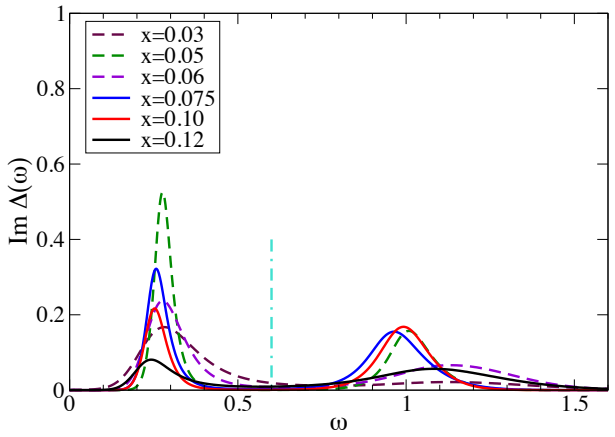

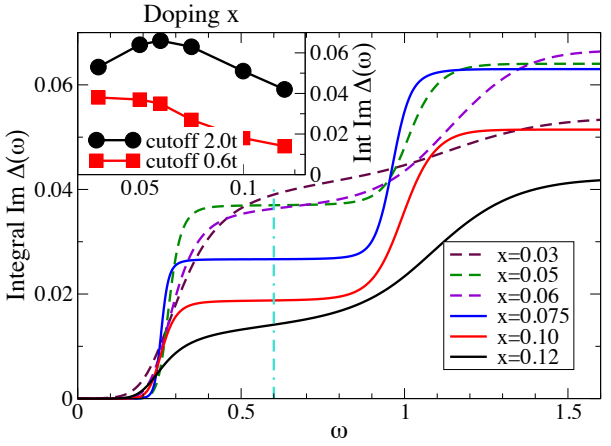

Acknowledgments

Many thanks to my collaborators:

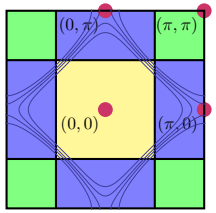

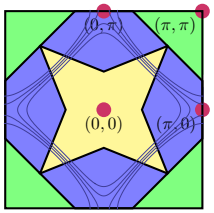

A. J. Millis
O. Parcollet

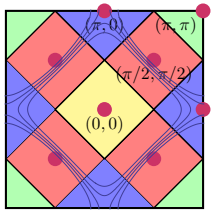

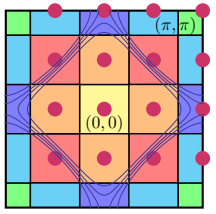

Emanuel Gull and Andrew J. Millis, arXiv:1407.0704
Emanuel Gull, Andrew J. Millis, Olivier Parcollet, Phys. Rev. Lett. 110, 216405 (2013)
Emanuel Gull and Andrew J. Millis, Phys. Rev. B 88, 075127 (2013)

Computer time: NERSC

Experiments: Momentum Space Differentiation

Overdoped Tl2201 / ADMR

Angle dependent magneto-resistance:

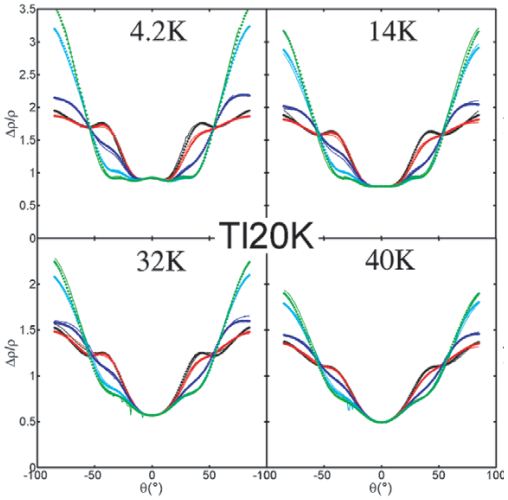

Data analysis:

$$\rho(T) = A + BT + CT^2$$

Angle dependent analysis:

$$\gamma_{\rm iso} \sim A + CT^2$$

$$\gamma_{\rm aniso} \sim BT(+CT^2)$$

Anisotropic component of scattering rate: maximal near antinodal point, minimal near nodal point.

Momentum space differentiation!

French, Analytis, Carrington, Balicas, Hussey: NJP 11, 05595 (2009)

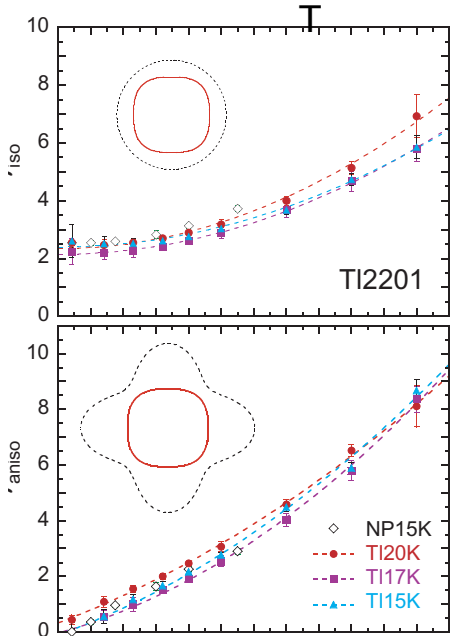

Figure 3. Temperature dependence of the isotropic (top panel) and anisotropic (middle panel) scattering rates determined from the ADMR measurements shown in figure 1. NP15K refers to the sample whose ADMR were measured at a single azimuthal angle [11]. The dashed lines in the top and middle panels are fits to $A + CT^2$ and $A + BT + CT^2$, respectively. The insets in each panel depict the Fermi surface (as red solid lines) and the corresponding scattering rates (as black dashed lines. Bottom panel: components of $\gamma_{\rm aniso}(T)$ (black long-dashed lines and green short-dashed lines) and $\gamma_{\rm iso}(T)$ (orange dots) for Tl15sK.

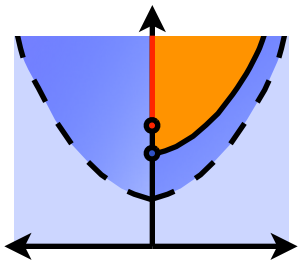

Momentum Space Differentiation

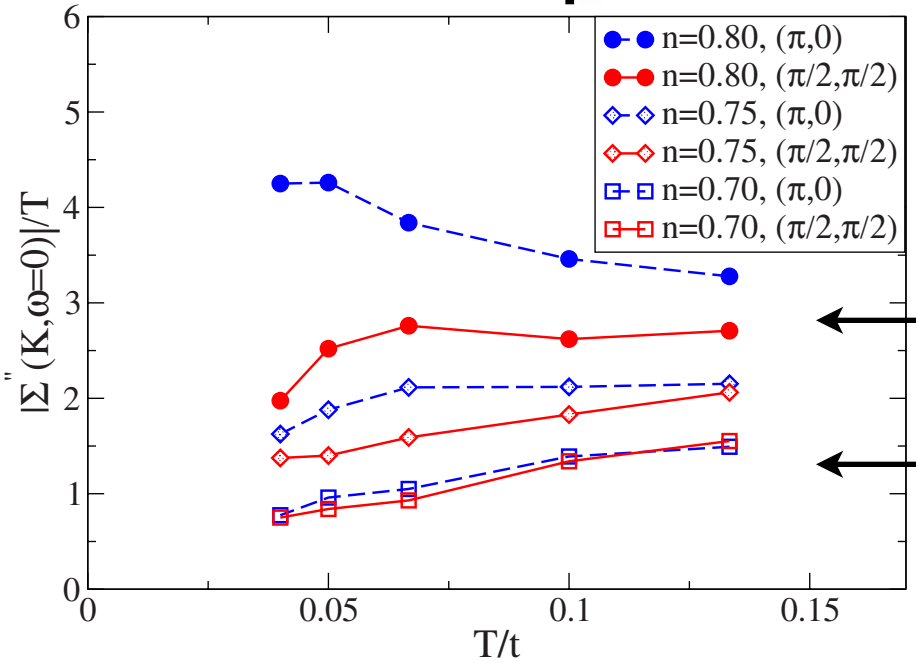

Red: Nodal scattering rates
Blue: Antinodal scattering rates

Momentum Space Differentiation

Isotropic Fermi Liquid regime

Momentum space differentiation (n ~ 0.8): Nodal scattering rate vanishing more rapidly than antinodal scattering rate, ~ linear behavior (slower than T^2)
Isotropic Fermi Liquid regime (n ~ 0.7): Nodal and Antinodal scattering rate identical, T^2

Similar to anisotropic component observed in Angle-Dependent Magneto-Resistance

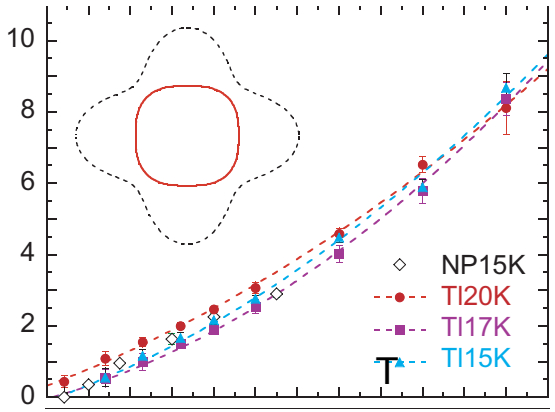

French, Analytis, Carrington, Balicas, Hussey: NJP 11, 05595 (2009)